

# Principled priors for Bayesian inference of circular models

Xiang Ye

Department of Statistics, King Abdullah University of science and technology  
and

Janet Van Niekerk

Department of Statistics, King Abdullah University of science and technology  
and

Håvard Rue

Department of Statistics, King Abdullah University of science and technology

February 11, 2026

## Abstract

Advancements in computational power and methodologies have enabled research on massive datasets. However, tools for analyzing data with directional or periodic characteristics, such as wind directions and customers' arrival time in 24-hour clock, remain underdeveloped. While statisticians have proposed circular distributions for such analyses, significant challenges persist in constructing circular statistical models, particularly in the context of Bayesian methods. These challenges stem from limited theoretical development and a lack of historical studies on prior selection for circular distribution parameters.

In this article, we propose a principled, practical and systematic framework for selecting priors that effectively prevents overfitting in circular scenarios, especially when there is insufficient information to guide prior selection. We introduce well-examined Penalized Complexity (PC) priors for the most widely used circular distributions. Comprehensive comparisons with existing priors in the literature are conducted through simulation studies and a practical case study. Finally, we discuss the contributions and implications of our work, providing a foundation for further advancements in constructing Bayesian circular statistical models.

*Keywords:* Directional Statistics, Circular Distribution, Penalised Complexity Prior

# 1 Introduction

Advancements in computational power have provided researchers with access to massive and diverse datasets across various fields, enabling the exploration of complex scientific and practical challenges. However, tools for analyzing data with complex structures, such as directional or periodic characteristics, remain underdeveloped, and many of these datasets require specialized methods for analysis. For instance, wind directions and bird migration paths are naturally represented on a compass, while hospital patient arrival times and passenger density fluctuations follow a 24-hour clock (Mardia & Jupp 2009). The orientation of earthquake epicenters, directions of cosmic rays and stellar objects in astronomy (Ley & Verdebout 2017, Pewsey & García-Portugués 2021, Cabella & Marinucci 2009), joint angles prone to injury, protein structure with angular measures in bioinformatics (Mardia et al. 2018, Boomsma et al. 2008), typhoon trajectories, and the analysis of angular components in multivariate extreme value statistics are additional examples of data that align with circular scales. These examples underscore the growing need for statistical frameworks capable of handling circular data.

Directional statistics offers appropriate tools for analyzing such data, with circular distributions — probability distributions defined on the circumference of a circle (Jammalamadaka 2001) and characterized by angular measures or radians — playing a central role. These methods are crucial for modeling data in fields such as meteorology, earth sciences, bioinformatics, ecology, medicine (Vuollo et al. 2016, Pardo et al. 2016), genetics, neurology, astronomy (Cabella & Marinucci 2009, Marinucci & Peccati 2011), image analysis (Jung et al. 2011, Esteves et al. 2018), text mining (Dhillon & Modha 2001, Banerjee et al. 2005), machine learning (Sra 2016), and beyond (Ley & Verdebout 2017, Pewsey & García-Portugués 2021).

Applying Bayesian methods to circular data, however, poses significant challenges, particularly in the selection of priors — a pivotal step in Bayesian analysis. Unlike Euclidean dis-

tributions, circular distributions have unique parameterizations and behaviors, often requiring specialized approaches. For example, in [Wallace & Dowe \(1993\)](#), priors for the concentration parameter  $\kappa$  of von Mises distribution are constructed through the techniques of Minimum Message Length (Section 2.1). These priors are also used in [Dowe et al. \(1996\)](#) and [Marrelec & Giron \(2024\)](#). Another popular prior for von Mises distribution is the joint conjugate prior proposed in [Damien & Walker \(1999\)](#). In addition, in the general procedure for Bayesian analysis with wrapped distributions proposed by [Ravindran & Ghosh \(2011\)](#), the Beta  $(a, a)$  prior is employed. [Nuñez-Antonio et al. \(2011\)](#) proposed to fit the Bayesian circular model through the projected normal distribution with normal priors. A prior for the location parameter is often more intuitive to formulate, while priors for the hyperparameters like dispersion parameters are notoriously hard to conceptualize. Moreover, when specific values of the hyperparameters result in model complexity reduction, care should be taken in the prior construction.

Since circular variables are defined on a compact and curved space rather than in linear Euclidean space, their geometric properties make it difficult to develop strong intuition about their behavior. This further complicates prior selection, increasing the risk of using priors that either dominate the posterior, or possibly lead to poorly performing models. Poorly chosen priors can cause overfitting in the Bayesian model. It is worth noting that *overfitting* in this article refers to the *Informal Definition 1* of [Simpson et al. \(2017\)](#), which defines a prior  $p(\xi)$  as *forcing overfitting* if it allocates insufficient mass to the *simpler model*, making it difficult for the posterior to recover a simpler model when supported by the data. A detailed discussion of the simpler model is presented in Section 3.1.

To address these challenges, we set two goals for this research. Firstly, we establish a principled framework for the hyperparameters of a general circular model, based on a simpler circular model. This framework is inspired by the Penalized Complexity (PC) prior framework proposed

by [Simpson et al. \(2017\)](#). The PC prior framework is a reliable choice for constructing default priors, which can balance model complexity and prior informativeness, particularly in scenarios with limited prior knowledge, when objective or uninformative priors are usually considered. Second, we derive the explicit expressions for the Penalized Complexity (PC) priors for the most commonly used circular distributions' hyperparameters and provide a way to quantify prior information through a user-defined parameter.

The structure of this paper is as follows: Section 2 reviews the most commonly used circular distributions, their properties, and existing priors in the literature. Section 3 introduces the proposed framework for prior selection and the procedure for deriving PC prior for circular distributions. Section 3.2 derives explicit formulations for widely used circular distributions. Section 4 evaluates the proposed priors through comparison studies and simulation studies, while Section 5 demonstrates their application to real-world datasets. Finally, Section 6 discusses broader implications and potential directions for future research.

## 2 Preliminaries

A proper circular distribution should have a probability density function  $p(x | \xi)$  that satisfies  $p(x | \xi) = p(x + 2\pi k | \xi)$  for any integer  $k$  and  $x \in [0, 2\pi)$ , where  $\xi$  is the parameters for the probability density function. Most circular distributions are constructed by using one of the following four general approaches: wrapping, conditioning, projection, and perturbation ([Ley & Verdebout 2017](#)).

Circular distributions in the wrapped family are constructed by taking a distribution defined on  $\mathbb{R}$  and wrapping it around a circle (modulus by  $2\pi$ , e.g. wrapped Normal distribution, wrapped Cauchy distribution, wrapped double exponential distribution); the conditioning approach obtains circular distributions through constructing joint distribution of polar coordinates (radius  $r$  and

angle  $\theta$ ) and finding the conditional distribution  $p(\theta | r)$  through restricting the radius  $r = 1$  (e.g. von Mises distribution); the projection approach projects an distribution on  $\mathbb{R}^2$  onto the unit circle (e.g. rejected Normal distribution); The perturbation approach provides flexible choices to extend a circular density to a more general form through multiplying it with a proper function (e.g. cardioid distribution). Details can be found in Chapter 2.2 of [Ley & Verdebout \(2017\)](#).

Notably, many of these distributions include the circular uniform distribution as a special case (Figure 1), defined by a probability density function given by  $p_U(x) = \frac{1}{2\pi}$ ,  $x \in [0, 2\pi)$ . Three

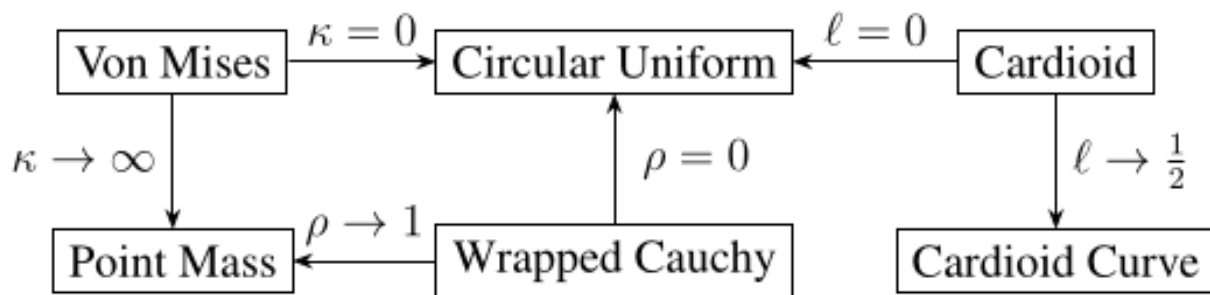


Figure 1: Relationship between popular circular distributions.  $\kappa$ ,  $\ell$  and  $\rho$  are the concentration parameters for von Mises, cardioid and wrapped Cauchy distributions.

of the most widely used circular distributions — the von Mises (vM) distribution, the cardioid distribution, and the wrapped Cauchy (WC) distribution — serve as the foundation for many generalizations and extensions in circular statistics ([Ley & Verdebout 2017](#)), such as the Jones-Pewsey distribution ([Jones & Pewsey 2005](#)) and the Kato-Jones distribution ([Kato & Jones 2010](#)), underscoring their importance in the field. One commonality between these three distributions is that they all include two parameters: one location parameter and one concentration parameter. The concentration parameter is essentially a scaling parameter for circular distributions. When data is distributed on a unit circle (or sphere/hypersphere), the concept of the standard deviation, as defined for linear data, becomes meaningless, since its interpretation is no longer clear, particularly when the standard deviation exceeds half a circle ( $\pi$ ). To describe the spread or sparsity of circular data, most circular distributions introduce a “concentration” parameter, which quan-

tifies the extent of concentration (or dispersion) within the data, indicating how densely the data are clustered around a mean direction (or how widely they are spread). In this work, we focus on the von Mises (vM) distribution, the cardioid distribution, and the wrapped Cauchy (WC) distribution, and on their Bayesian inference.

## 2.1 Von Mises Distribution

The *von Mises distribution* (Mardia & Jupp 2009), often referred to as the *circular normal distribution* (Gumbel et al. 1953), is the circular analogue of the normal distribution. It is one of the most widely used and versatile circular distributions (Mardia & Jupp 2009). Its probability density function is given by:

$$p_{\mathcal{VM}}(x \mid \mu, \kappa) = \frac{1}{2\pi \mathcal{I}_0(\kappa)} \exp \{ \kappa \cos(x - \mu) \}, \quad \mu \in [0, 2\pi), \quad \kappa \in [0, \infty), \quad (1)$$

where  $\mu$  is the location parameter,  $\mathcal{I}_a(\cdot)$  is the modified Bessel function of the first kind of order  $a \in \mathbb{N}$ , and  $\kappa$  is the concentration parameter. The plot for this density is given in Figure 2. The von

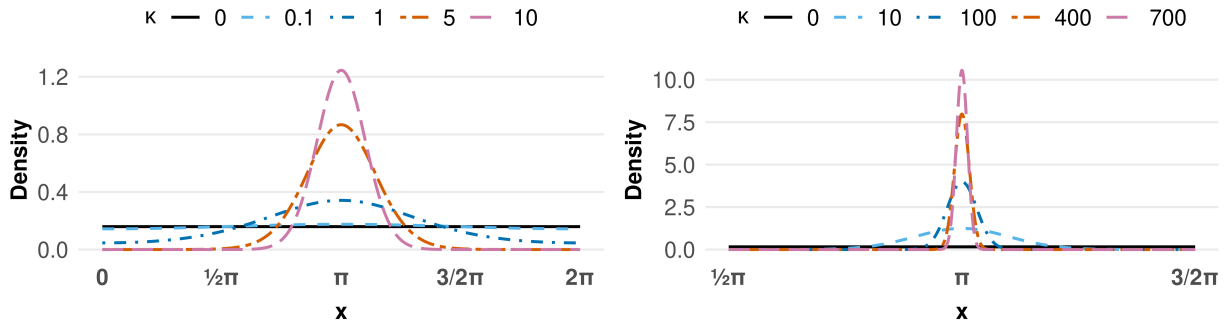


Figure 2: vM density for small (left) and large (right)  $\kappa$  values with  $\mu = \pi$ .

Mises distribution includes the circular uniform distribution as a special case when  $\kappa = 0$ , while  $\kappa \rightarrow \infty$  indicates that the data are highly concentrated around the mean direction  $\mu$ . Thus,  $\kappa$  can be interpreted as analogous to the precision of the normal distribution ( $1/\sigma^2$ ). Since the Gamma

distribution is a common prior choice for the precision in normal distributions, the Gamma  $(a, b)$  distribution with density given in Equation 2 is naively considered as a prior for  $\kappa$ .

$$p(x | a, b) = \frac{b^a}{\Gamma(a)} x^{a-1} \exp\{-bx\} \quad (2)$$

[Guttorp & Lockhart \(1988\)](#) proposed a joint conjugate prior for  $\mu$  and  $\kappa$ , expressed as:

$$p(\mu, \kappa) \propto [\mathcal{I}_0(\kappa)]^{-c} \exp\{\kappa R_0 \cos(x - \mu_0)\} \quad (3)$$

where  $c$ ,  $R_0$  and  $\mu_0$  are prior hyperparameters. When  $c \in \mathbb{N}$ ,  $c$  can be interpreted as representing  $c$  prior observations concentrated around the direction  $\mu_0$ , with  $R_0$  corresponding to the component of the resultant vector in the known direction ([Damien & Walker 1999](#)).

Despite its intuitive interpretation, deriving the posterior distribution under this prior requires introducing additional hyperparameters and several latent variables during the sampling process (see [Damien & Walker 1999](#) for details). This construction, however, increases computational complexity and often results in greater Monte Carlo variability of the posterior estimates, owing to the mixing and dependence among latent components. In some cases, particularly when  $c$  and  $R_0$  are not well chosen, or when their combinations convey weak prior information, it may also lead to wider posterior credible intervals.

[Dowe et al. \(1996\)](#) and [Marrelec & Giron \(2024\)](#) both considered two different priors for  $\kappa$  originally proposed by [Wallace & Dowe \(1993\)](#) derived from minimum message length (MML). These priors are defined as:

$$h_2(\kappa) = \frac{2}{\pi(1 + \kappa^2)} \quad \text{and} \quad h_3(\kappa) = \frac{\kappa}{(1 + \kappa^2)^{3/2}}. \quad (4)$$

Minimum Message Length (MML) is a Bayesian information-theoretic restatement of Occam's

razor, favoring models that describe the data most efficiently. It encodes both the model and the data as one message, where a more complex model requires a longer description and is only preferred if it leads to a shorter overall message. In this sense, priors derived from MML, such as  $h_2(\kappa)$  and  $h_3(\kappa)$ , naturally penalize overly complex or highly concentrated models unless the data provide strong evidence to support them.

## 2.2 Cardioid Distribution

The *cardioid distribution* is a cardioid perturbation of the circular uniform distribution (Ley & Verdebout 2017) with probability density function given by

$$p_C(x | \mu, \ell) = \frac{1}{2\pi} (1 + 2\ell \cos(x - \mu)), \quad \mu \in [0, 2\pi), \quad \ell \in [0, 1/2]. \quad (5)$$

Here,  $\ell$  is the concentration parameter which controls the deviation from the circular uniform distribution. Larger values of  $\ell$  result in stronger departures from uniformity (see the left-hand-side plot in Figure 3). It is obvious from the plot that the cardioid density is much less concentrated compared with the von Mises density, even when the concentration parameter  $\ell$  for the former density approaches its supremum. This property enables the cardioid distribution to be more appropriate for dispersed data (heavy-tailed data) compared with von Mises distribution. Thus, the cardioid distribution is primarily used as a small concentration approximation to the von Mises distribution, as noted by Mardia & Jupp (2009). Two reasonable prior choices for  $\ell$  could be the Uniform  $(0, 0.5)$  prior and the  $0.5 \times \text{Beta}(a, b)$  prior, since both priors fit the requirement of support being  $[0, 0.5)$ .

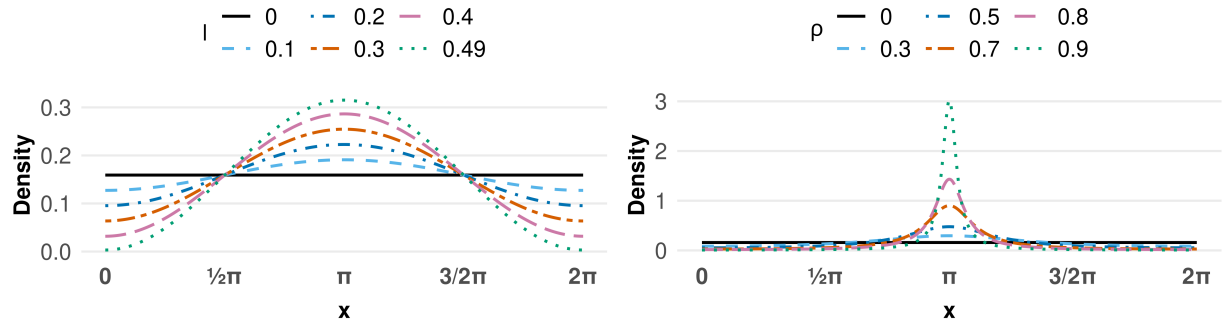


Figure 3: Cardioid density (left) and wrapped Cauchy density (right) with  $\mu = \pi$  for different concentration parameter values.

### 2.3 Wrapped Cauchy Distribution

The wrapped Cauchy distribution is one of the rare wrapped distribution that has an analytic density function, since its probability density can be expressed in closed form (Ley & Verdebout 2017). Further details of the WC distribution are discussed in Chapter 3.5.7 of Mardia & Jupp (2009). The probability density function is given by:

$$p_{WC}(x | \mu, \rho) = \frac{1}{2\pi} \frac{1 - \rho^2}{1 + \rho^2 - 2\rho \cos(x - \mu)}, \quad \text{where } \mu \in [0, 2\pi), \quad \rho \in [0, 1). \quad (6)$$

The parameter  $\rho$  serves as a measure of concentration, with  $\rho = 0$  corresponding to the circular uniform distribution, indicating no concentration and as  $\rho \rightarrow 1$ , the data become increasingly concentrated, converging to a point mass distribution. The density plot for different  $\rho$  values is given in the right-hand side of Figure 3.

For Bayesian analysis with a WC distribution, one reasonable choice for the prior for  $\rho \in [0, 1]$  is a Beta( $a, b$ ) prior, which has support in  $[0, 1]$ . Ravindran & Ghosh (2011) mentioned that Beta( $a, a$ ) is a class of non-informative priors for  $\rho$ . However, the beta prior behaves markedly differently with different choices for  $a$  and  $b$ , and therefore they need to be chosen carefully.

The circular distributions and priors discussed above highlight the diversity and utility of existing methods for modeling circular data. However, many of the priors currently in use are

either heuristic or tailored to specific cases, lacking a unified framework. This motivates the need for a principled approach for prior selection which can account for the unique properties of circular distributions, which we present in the next section.

### 3 Methodology

This section introduces a principled framework for constructing hyperpriors for circular distributions that favors simpler circular models. The guiding principles, along with the corresponding prior formulation framework that satisfies them, are presented in Section 3.1, and specific priors for widely used circular distributions are proposed in Section 3.2.

#### 3.1 Penalizing complexity prior for circular models

When there is no sufficient information supporting that the data require a complicated model, following the principle of *Occam's razor*, it is necessary to examine model complexity when setting a prior. One effective way to penalize Bayesian model complexity is through the selection of a proper prior distribution, ensuring that the prior exerts a reasonable influence on the model's complexity. With this motivation, [Simpson et al. \(2017\)](#) proposed the PC prior framework, built upon four principles: *Occam's razor*, *measure of complexity*, *constant rate penalization* and *user-defined scaling*. The *measure of complexity* principle states that the prior should be constructed using a model complexity measure defined by the “distance”  $d$  between the model of interest and a simpler base model; The *constant rate penalization* principle specifies that the PC prior density decays at a constant rate  $r \in (0, 1)$  with respect to an increment  $\delta$  in the distance  $d$ , satisfying

$$\frac{p_d(d + \delta)}{p_d(d)} = r^\delta, \quad d, \delta \geq 0. \quad (7)$$

Finally, the *user-defined scaling* principle suggests that users should have at least some understanding of the data, or of how complex the model is expected to be, to define the strength of penalization accordingly.

The PC prior framework has been successfully applied across a wide range of fields, demonstrating both its practicality and robustness. For instance, it has been widely used in spatial and spatio-temporal modelling (Fuglstad et al. 2019, Cabral et al. 2023, Rodriguez Avellaneda et al. 2025), time-series analysis (Sørbye & Rue 2017), survival modelling (Van Niekerk et al. 2021), and nonparametric regression (Ventrucci & Rue 2016). These applications highlight the flexibility of PC priors in controlling model complexity across diverse modelling contexts, motivating their extension to circular data.

In Euclidean space, statistical measures such as standard deviation and variance are intuitive and straightforward in terms of interpretability. However, as discussed in Section 2, these quantities lose their intuitive meanings for data collected on a circular domain (or transformed into circular form) and concentration parameters are used. The parameterization of the concentration parameter varies among circular distributions but typically includes the value “0” as a special case, representing no concentration (or maximum dispersion). In most common cases, the distribution is simplified to the circular uniform distribution. It should be noted that the mean direction is not likelihood identifiable in the circular uniform distribution.

In contrast, as the concentration parameter increases, most circular distributions tend toward a point mass, representing extreme concentration around a specific direction (mean). An exception is the cardioid distribution which tends toward a cardioid curve rather than collapses into a point mass.

Although most circular distributions exhibit desirable properties when their concentration parameters approach the boundary values, the inference for these distributions can be unstable

because the data are defined on a limited range ( $[0, 2\pi)$ ). As a result, small variations in the data can correspond to large changes on the circular scale, making the concentration parameter highly sensitive. In particular, when the data deviate from the boundary cases, that is, when they are neither strongly clustered nor close to circular uniformity, the underlying model structure becomes more complex and the estimation of the concentration parameters becomes difficult and less stable.

This sensitivity and instability highlight the need for a principled approach to regularizing model complexity. One natural way to achieve this is to view the boundary cases as simpler circular models, which can be regarded as the “*base model*” in the PC prior framework, that is, the simplest models representing minimal structure and the most straightforward interpretation. The notion of model complexity can then be described by the *measure of complexity* principle, where the model complexity is quantified as the distance from the base model. We let  $p(x | \xi)$  be the model of interest, where  $x$  is the data and  $\xi$  is the parameter of interest, and let  $p(x | \xi_0)$  represent the base model, with  $\xi = \xi_0$  be the corresponding parameter value at the base model. [Simpson et al. \(2017\)](#) proposed a reasonable distance measure, and in circular scenarios it can be written as

$$d(\xi) = \sqrt{\text{KLD}(p(x | \xi) || p(x | \xi_0))} = \sqrt{\int_0^{2\pi} p(x | \xi) \log \left( \frac{p(x | \xi)}{p(x | \xi_0)} \right) dx}, \quad (8)$$

where  $\text{KLD}(\cdot || \cdot)$  denotes the Kullback-Leibler divergence (KLD) ([Kullback & Leibler 1951](#)) between two distributions, which is one of the most widely used quantitative measures of the difference between probability distributions.

Following the formulation of [Simpson et al. \(2017\)](#), the Penalized Complexity (PC) prior for a model parameter  $\xi$  is defined as an exponential probability density function with respect to the

distance, as follows:

$$p(d) = \lambda \exp\{-\lambda d\} \iff p(\xi) = \lambda \exp\{-\lambda d(\xi)\} \left| \frac{\partial d(\xi)}{\partial \xi} \right|. \quad (9)$$

where  $\lambda$  is the scaling parameter of the PC prior, defined such that  $P_{\mathcal{PC}}(Q(\xi) > U) = \alpha$ , with  $Q(\xi)$  being a function of  $\xi$ ,  $U$  being a reasonable value of  $Q(\xi)$  and  $\alpha \in (0, 1)$  a value representing probability. The formulations of  $Q(\xi)$  are discussed later in this section.

To illustrate how the PC prior behaves with respect to the distance measure, Figure 4 is presented. The left-hand-side plot shows the distance  $d(\kappa)$  between the von Mises distribution and the circular uniform distribution. If we express the prior density for  $\kappa$ ,  $p(\kappa)$ , in terms of distance,  $p(d)$ , then from the right-hand-side plot of Figure 4, we can observe that the prior density decreases as the distance increases. Since PC priors are exponential with respect to distance, for any concentration parameter  $\xi$  of a circular distribution, the density of its PC prior will always be penalized as the distance between that circular distribution and the base model increases. Moreover, because the prior is defined to be exponential on the distance scale, this penalization occurs at a constant rate with respect to increments in distance. Therefore, the PC prior satisfies the *constant rate penalization* principle, and inherently favors simpler models, penalizing the prior density exponentially as the distance  $d(\xi)$  increases. The scaling parameter,  $\lambda$ , of the PC prior

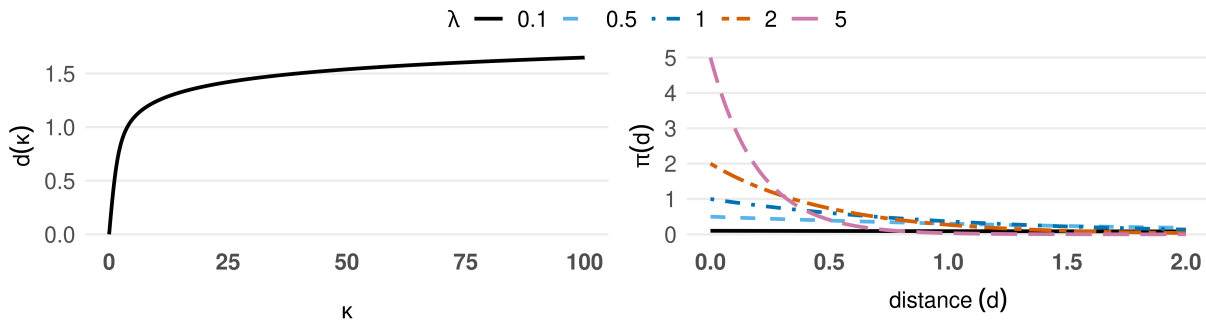


Figure 4: Distance ( $d(\kappa)$ ) between vM distribution and circular uniform distribution (left) and the PC prior density in distance scale for different  $\lambda$  values (right).

determines the strength of penalization for deviations away from the base model. To satisfy the *ser-defined scaling* principle and to appropriately select the scaling parameter, users need to have some understanding of the data and its properties. A general strategy for selecting  $\lambda$  is to set  $Q(\xi) = \psi$ , where  $\psi \in [0, 1]$  denotes the *mean resultant length*. Following [Ley & Verdebout \(2017\)](#) and [Lund et al. \(2017\)](#), it is defined as

$$\psi = \frac{1}{n} \sqrt{\left(\sum_{i=1}^n \cos(x_i)\right)^2 + \left(\sum_{i=1}^n \sin(x_i)\right)^2}, \quad (10)$$

for data  $x_i, i = 1, 2, \dots, n$ . Alternative definitions of this quantity also exist, such as moving the factor  $\frac{1}{n}$  inside the two squared summations ([Mardia & Jupp 2009](#)). This quantity is a measure of the concentration around the circle. A value of  $\psi = 0$  corresponds to a circular uniform distribution where there is no preferred direction, while  $\psi = 1$  indicates that all observations coincide at the same angle (maximum concentration). Under this interpretation,  $P_{PC}(Q(\xi) > U) = \alpha$  expresses the belief that “*the probability that the mean resultant length of the data exceeds  $U$ , is  $\alpha$* ”.

This interpretation is model-independent, as the user can also express  $\psi$  explicitly as a function of the model parameter  $\xi$ , and therefore interpret  $Q(\xi)$  in terms of  $\xi$ . For instance, in the von Mises distribution,  $\psi(\kappa) = \frac{I_1(\kappa)}{I_0(\kappa)}$ , whilst for the cardioid and wrapped Cauchy distributions,  $\psi$  equals to the concentration parameters  $\ell$  and  $\rho$  respectively. Conceptually, the mean resultant length serves as a sample-based indicator of data concentration, while the concentration parameter of a circular distribution controls the shrinkage behavior of the corresponding probability density. Therefore, the mean resultant length links the circular distribution to the observed data, incorporating the information from the data into the density function.

This unified approach covers various circular models under one framework. However, it may not be intuitive for users inexperienced with circular data. Therefore, an alternative, more

intuitive approach is also suggested.

For most circular distributions, where the bounds of the concentration parameter  $\xi$  correspond to the circular uniform distribution and a point mass, a suitable transformation  $Q(\xi)$  can often be found. For instance, one could define  $Q(\xi)$  such that circular uniform density corresponds to  $Q(\xi) \rightarrow 2\pi$ , and the point mass corresponds to  $Q(\xi) \rightarrow 0$ . Under this transformation,  $Q(\xi) \in (0, 2\pi)$ , making  $P_{PC}(Q(\xi) > U) = \alpha$  represent “the probability that the data fall outside a radian  $U$  around the mean direction being equal to  $\alpha$ ”. The small values of  $U$  indicate a high concentration to a point mass, whilst large values of  $U$  mean that the user believes the data spread widely. This transformation is intuitive and allows users to gain insights into appropriate values for  $U$  and  $\alpha$  by visualizing the data.

It is worth noting that the proposed PC priors are flexible in terms of informativeness. That is, they can be either weakly or strongly informative (Simpson et al. 2017), depending on the user’s belief about the data. As an illustration, consider selecting the value of  $\lambda$  using the mean resultant length ( $Q(\xi) = \psi$ ). If the user believes that “the mean resultant length of the data is nearly impossible to be higher than 0.8,” then one can set  $U = 0.8$  and  $\alpha = 0.001$  to obtain a strongly informative prior. Conversely, if the user has no prior knowledge about the concentration of the data,  $\lambda$  can be chosen by setting  $U = 0.5$  and  $\alpha = 0.5$ , indicating uncertainty about whether the mean resultant length of the data should be larger or smaller than the median, which consequently yields a weakly informative prior. Therefore, the PC prior can always be employed regardless of whether sufficient prior information is available.

## 3.2 Specific cases

### 3.2.1 Von Mises Distribution

The first step in deriving the PC prior is to compute the KLD. For the vM distribution as defined in Equation 1, the KLD is given below:

$$\begin{aligned} \text{KLD}(\mathcal{VM} \parallel \mathcal{VM}_0) &= \int_0^{2\pi} p(x \mid \mu, \kappa) \log \left( \frac{p(x \mid \mu, \kappa)}{p(x \mid \mu, \kappa_0)} \right) dx \\ &= \log(\mathcal{I}_0(\kappa_0)) - \log(\mathcal{I}_0(\kappa)) + \frac{\kappa \mathcal{I}_1(\kappa)}{\mathcal{I}_0(\kappa)} - \frac{\kappa_0 \mathcal{I}_1(\kappa)}{\mathcal{I}_0(\kappa)}. \end{aligned} \quad (11)$$

Recall the behavior of the vM density with respect to changes in the concentration parameter  $\kappa$  (Section 2.1). Two natural choices for base model for the concentration parameter are the circular uniform distribution ( $\kappa_0 = 0$ ), representing no concentration, and the point mass ( $\kappa_0 \gg \kappa$ ), representing high concentration. With these two chosen base models, the corresponding PC priors for  $\kappa$  can be computed and are given in Proposition 3.1 and Proposition 3.2 respectively. The proofs are given in Appendix A.1.

**Proposition 3.1.** *The PC prior for concentration parameter  $\kappa$  of the von Mises distribution with the base model at  $\kappa_0 = 0$  has density*

$$p(\kappa) = \lambda \exp \left\{ -\lambda \sqrt{\frac{\kappa \mathcal{I}_1(\kappa)}{\mathcal{I}_0(\kappa)} - \log(\mathcal{I}_0(\kappa))} \right\} \frac{\frac{\kappa(\mathcal{I}_0(\kappa) + \mathcal{I}_2(\kappa))}{2\mathcal{I}_0(\kappa)} - \frac{\kappa \mathcal{I}_1(\kappa)^2}{\mathcal{I}_0(\kappa)^2}}{2 \sqrt{\frac{\kappa \mathcal{I}_1(\kappa)}{\mathcal{I}_0(\kappa)} - \log(\mathcal{I}_0(\kappa))}}, \quad (12)$$

where  $\lambda > 0$ , and the corresponding CDF is

$$F(\kappa) = 1 - \exp \left\{ -\lambda \sqrt{\frac{\kappa \mathcal{I}_1(\kappa)}{\mathcal{I}_0(\kappa)} - \log(\mathcal{I}_0(\kappa))} \right\}. \quad (13)$$

**Proposition 3.2.** *The PC prior for concentration parameter  $\kappa$  of the von Mises distribution with*

the base model at  $\kappa_0 \gg \kappa$  has density

$$p(\kappa) = \lambda \exp \left\{ -\lambda \sqrt{1 - \frac{\mathcal{I}_1(\kappa)}{\mathcal{I}_0(\kappa)}} \right\} \frac{\frac{\mathcal{I}_0(\kappa) + \mathcal{I}_2(\kappa)}{2\mathcal{I}_0(\kappa)} - \frac{\mathcal{I}_1(\kappa)^2}{\mathcal{I}_0(\kappa)^2}}{2\sqrt{1 - \frac{\mathcal{I}_1(\kappa)}{\mathcal{I}_0(\kappa)}}}, \quad (14)$$

where  $\lambda > 0$ , and the corresponding CDF is

$$F(\kappa) = \exp \left\{ -\lambda \sqrt{1 - \frac{\mathcal{I}_1(\kappa)}{\mathcal{I}_0(\kappa)}} \right\}. \quad (15)$$

The plots for the density of both PC prior and the corresponding log-log density are presented in Figure 5 (prior with  $\kappa_0 = 0$  base model) and Figure 6 (prior with  $\kappa_0 \rightarrow \infty$  base model). The plots show that both PC priors vary with the value of scaling parameter  $\lambda$ . For the PC prior with the base model being circular uniform density ( $\kappa_0 = 0$ ), the prior density reaches the peak at  $\kappa = 0$ , which indicates that this prior prefers a more uniformly distributed model. As for the PC prior with the base model being a point mass (Figure 6), it assigns more density away from  $\kappa = 0$  when  $\lambda$  increases. In other words, this PC prior believes that the data are more concentrated compared with the PC prior with circular uniform base model. Since  $\kappa \in [0, \infty)$ , following the

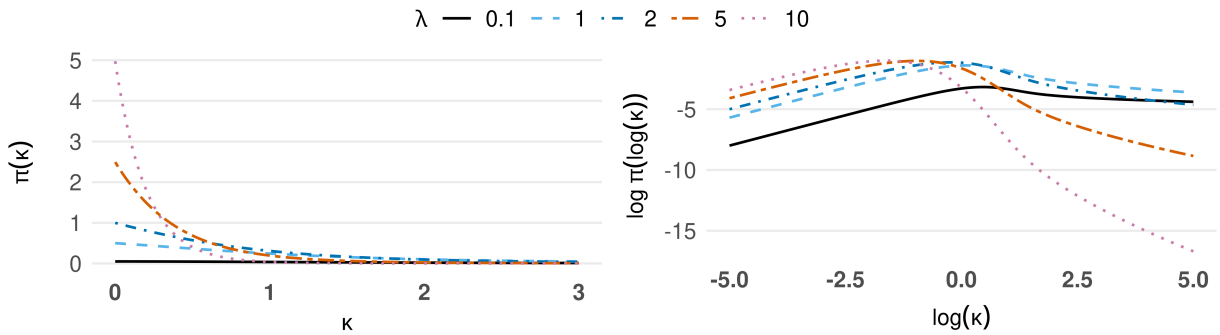


Figure 5:  $\kappa_0 = 0$  base model PC prior density (left) and log-log density (right).

discussion on interpretable transformation in Section 3.1, we suggest the transformation  $Q(\kappa) = \frac{2\pi}{1+\kappa} \in [0, 2\pi]$ , which represents the radian of a circle. Therefore, the scaling parameter  $\lambda$  for the PC prior for the concentration parameter of von Mises distribution can be computed and

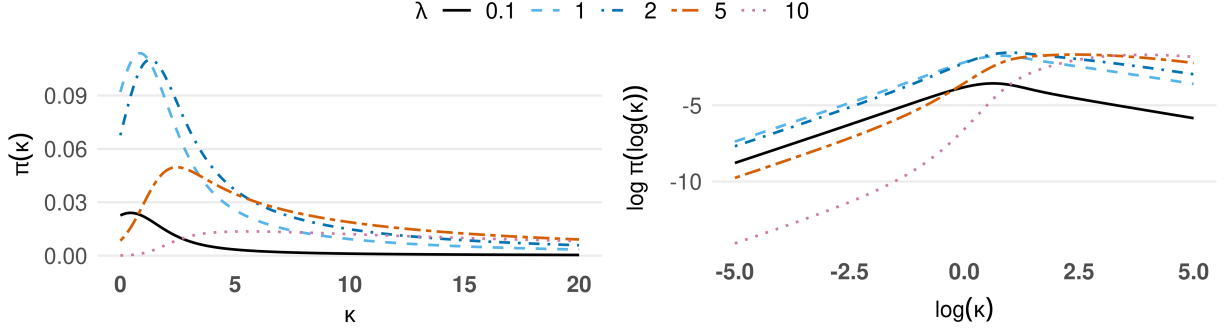


Figure 6:  $\kappa_0 \rightarrow \infty$  base model PC prior density (left) and log-log density (right).

calibrated by

$$P(Q(\kappa) > U) = P\left(\frac{2\pi}{1+\kappa} > U\right) = P\left(\kappa < \frac{2\pi}{U} - 1\right) = F\left(\frac{2\pi}{U} - 1\right) = \alpha. \quad (16)$$

Therefore, the expressions for computing  $\lambda$  for PC priors for  $\kappa$  are given by

$$\lambda = \begin{cases} -\frac{\log(1-\alpha)}{\sqrt{\frac{(\frac{2\pi}{U}-1)\mathcal{I}_1(\frac{2\pi}{U}-1)}{\mathcal{I}_0(\frac{2\pi}{U}-1)} - \log(\mathcal{I}_0(\frac{2\pi}{U}-1))}} & \text{for base model at } \kappa_0 = 0; \\ -\frac{\log(1-\alpha)}{\sqrt{1 - \frac{\mathcal{I}_1(\frac{2\pi}{U}-1)}{\mathcal{I}_0(\frac{2\pi}{U}-1)}}} & \text{for base model at } \kappa_0 \rightarrow \infty. \end{cases} \quad (17)$$

### 3.2.2 Cardioid Distribution

For the cardioid distribution as defined in (5), we have the KLD as

$$\begin{aligned} \text{KLD}(\mathcal{C}||\mathcal{C}_0) &= \int_0^{2\pi} p(x|\mu, \ell) \log\left(\frac{p(x|\mu, \ell)}{p(x|\mu, \ell_0)}\right) dx \\ &= 1 - \sqrt{1 - 4\ell^2} - \frac{\ell}{\ell_0} \left(1 - \sqrt{1 - 4\ell_0^2}\right) + \log(\ell) - \log(\ell_0) \\ &\quad + \frac{1}{2} \log\left(1 + \sqrt{1 - 4\ell^2}\right) - \frac{1}{2} \log\left(1 - \sqrt{1 - 4\ell^2}\right) \\ &\quad + \frac{1}{2} \log\left(1 - \sqrt{1 - 4\ell_0^2}\right) - \frac{1}{2} \log\left(1 + \sqrt{1 - 4\ell_0^2}\right). \end{aligned} \quad (18)$$

The base models for the concentration parameter  $\ell$  of cardioid distribution are unusual, as  $\ell$  controls the extent of the cardioid curve deviating away from the circular uniform distribution. Therefore, the two base models for  $\ell$  are the circular uniform distribution  $\ell_0 = 0$  and the most un-uniform cardioid curve ( $\ell_0 \rightarrow \frac{1}{2}$ ), and the corresponding PC prior for  $\ell$  are given in Proposition 3.3 and Proposition 3.4. The proofs are given in Appendix A.2.

**Proposition 3.3.** *The PC prior for concentration parameter  $\ell$  of the cardioid distribution with the base model at  $\ell_0 = 0$  has density*

$$p(\ell) = \lambda \exp\{-\lambda d(\ell)\} \frac{2\ell}{\left(1 - \exp\left\{-\lambda\sqrt{1 - \log(2)}\right\}\right) (1 + \sqrt{1 - 4\ell^2}) d(\ell)}, \quad (19)$$

where  $\lambda > 0$ , and

$$d(\ell) = \sqrt{1 - \sqrt{1 - 4\ell^2} + \log(\ell) + \frac{1}{2} \log\left(\frac{1 + \sqrt{1 - 4\ell^2}}{1 - \sqrt{1 - 4\ell^2}}\right)}. \quad (20)$$

The corresponding CDF is

$$F(\ell) = \frac{1 - \exp\{-\lambda d(\ell)\}}{1 - \exp\left\{-\lambda\sqrt{1 - \log(2)}\right\}}. \quad (21)$$

**Proposition 3.4.** *The PC prior for concentration parameter  $\ell$  of the cardioid distribution with the base model at  $\ell_0 \rightarrow \frac{1}{2}$  has density*

$$p(\ell) = \lambda \exp\{-\lambda d(\ell)\} \frac{2\ell + \sqrt{1 - 4\ell^2} - 1}{2\ell d(\ell)}, \quad (22)$$

where  $\lambda > 0$ , and

$$d(\ell) = \sqrt{1 + \log(2) - 2\ell - \sqrt{1 - 4\ell^2} + \log(\ell) + \frac{1}{2} \log\left(\frac{1 + \sqrt{1 - 4\ell^2}}{1 - \sqrt{1 - 4\ell^2}}\right)}. \quad (23)$$

The corresponding CDF is

$$F(\ell) = \exp\{-\lambda d(\ell)\}. \quad (24)$$

The plots for the density of both PC prior and the respected log-log density are presented in Figure 7 (prior with  $\ell_0 = 0$  base model) and Figure 8 (prior with  $\ell_0 \rightarrow 0.5$  base model). Figure 7 illustrates that the PC prior with a uniform base model assigns higher density at  $\ell = 0$  for larger values of  $\lambda$ . However, there is always a sharp increase in density as  $\ell \rightarrow 0.5^-$ . In contrast, for the PC prior with  $\ell_0 \rightarrow 0.5$  as the base model (Figure 8), the prior density increases monotonically with  $\ell$ . Additionally, the rate of increase becomes steeper as  $\ell$  approaches 0.5. The parameter

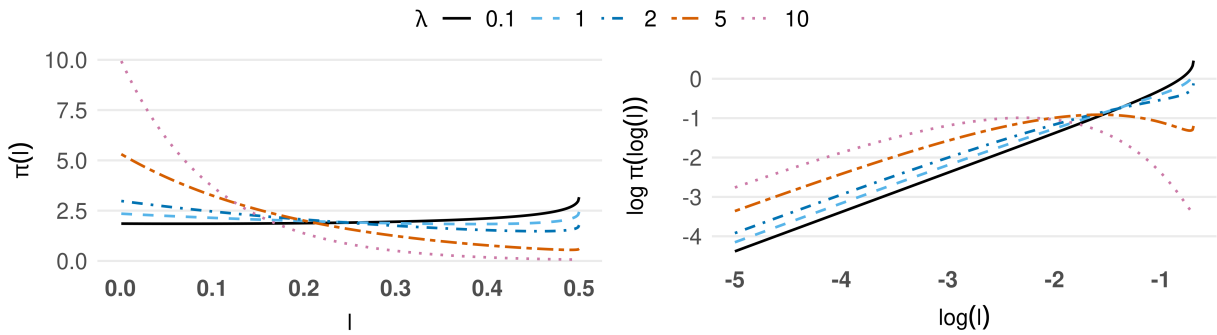


Figure 7:  $\ell_0 = 0$  base model PC prior density (left) and log-log density (right).

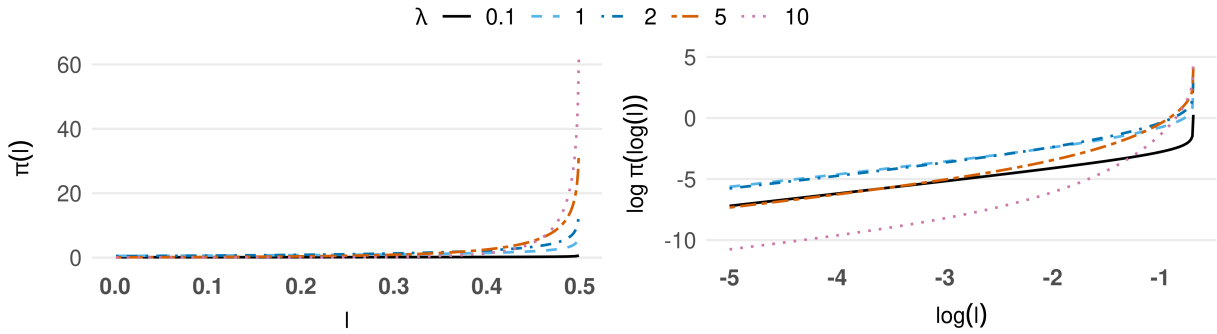


Figure 8:  $\ell_0 \rightarrow 0.5$  base model PC prior density (left) and log-log density (right).

$\ell$  serves as a shape-concentration parameter, controlling the “cardioidity” of the density. Unlike the von Mises (vM) and wrapped Cauchy (WC) distributions, it is not appropriate to define  $Q(\ell)$  using similar ideas due to the unique role of  $\ell$  in determining the cardioid shape. Instead, we

propose the transformation  $Q(\ell) = 2\ell \in (0, 1)$ , which provides a meaningful interpretation as the “cardiodity rate” from 0 to 1. Using this transformation, the scaling parameter  $\lambda$  in Equation 22 can be calculated by solving:

$$P(Q(\ell) > U) = P(2\ell > U) = P\left(\ell > \frac{U}{2}\right) = 1 - F\left(\frac{U}{2}\right) = \alpha \quad (25)$$

This transformation ensures an intuitive and interpretable way to set  $U$ , representing the threshold for the “cardiodity rate” and  $\alpha$ , which controls the weight assigned to the tail of the PC prior.

Through calculation, the expressions for computing  $\lambda$  for PC priors for  $\kappa$  are given by

$$\lambda = \begin{cases} -\frac{\log(\alpha + (1-\alpha)\exp\{-\lambda\sqrt{1-\log 2}\})}{d(\frac{U}{2})} & \text{for base model at } \ell_0 = 0; \\ -\frac{\log(1-\alpha)}{d(\frac{U}{2})} & \text{for base model at } \ell_0 \rightarrow \frac{1}{2}, \end{cases} \quad (26)$$

where  $d(\cdot)$  for both cases are given in Proposition 3.3 and Proposition 3.4 respectively.

### 3.2.3 Wrapped Cauchy Distribution

Recall that  $\rho = 1$  is not well defined for the wrapped Cauchy density (Section 2.3), and also that the WC distribution is preferred as a model with less concentration, when compared with vM distribution. WC distribution is thus usually employed when we believe the data are not strongly concentrated. Thus, it is more reasonable to consider the circular uniform distribution ( $\rho_0 = 0$ ) as the only base model for concentration parameter  $\rho$  of the WC distribution. Therefore, the KLD

between  $p(x | \mu, \rho)$  and  $p(x | \mu, \rho_0 = 0)$  is

$$\begin{aligned} \text{KLD}(\mathcal{WC} \parallel \mathcal{WC}_0) &= \int p(x | \mu, \rho) \log \left( \frac{p(x | \mu, \rho)}{p(x | \mu, \rho_0)} \right) dx \\ &= -\log(1 - \rho^2) - \log(1 - \rho_0^2) + 2 \log(1 - \rho_0 \rho) \\ &= -\log(1 - \rho^2) \end{aligned} \quad (27)$$

With this result, the PC prior for  $\rho$  is given in Proposition 3.5.

**Proposition 3.5.** *The PC prior for concentration parameter  $\rho$  of the wrapped Cauchy distribution with the base model at  $\rho_0 = 0$  has density*

$$p(\rho) = \lambda \exp \left\{ -\lambda \sqrt{-\log(1 - \rho^2)} \right\} \frac{\rho}{(1 - \rho^2) \sqrt{-\log(1 - \rho^2)}}, \quad (28)$$

where  $\lambda > 0$ , and the corresponding CDF is

$$F(\rho) = 1 - \exp \left\{ -\lambda \sqrt{-\log(1 - \rho^2)} \right\}. \quad (29)$$

The proof is provided in Appendix A.3, and the density and log-log density plots of this PC prior are shown in Figure 9. The density plot indicates that higher values of  $\lambda$  result in greater prior density at  $\rho = 0$ , and the prior density increases sharply as  $\rho$  approaches 1. In the log-log scale, the prior behavior reveals a consistent trend across different values of  $\lambda$ , suggesting similar characteristics despite variations in  $\lambda$ . Although the point mass boundary for WC distribution  $\rho = 1$  is not well-defined,  $\rho$  still controls the concentration behavior of the distribution from uniform to approximate point mass. Therefore, to compute the scaling parameter of the PC prior, the same idea of interpretable transformation for a parameter could be employed. For  $\rho \in [0, 1)$ , we propose to use the transformation  $Q(\rho) = 2\pi(1 - \rho) \in [0, 2\pi]$ . Now,  $Q(\rho) \rightarrow 2\pi$  when

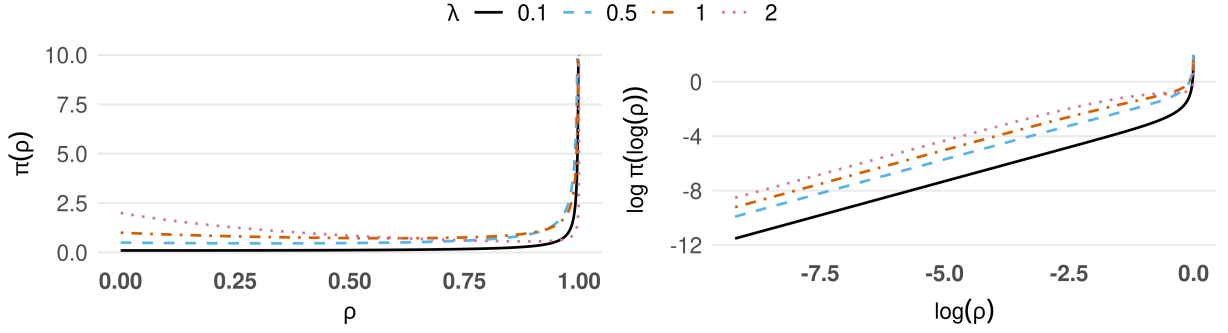


Figure 9: PC prior (for  $\rho$ ) density (left) and log-log density (right).

$\rho \rightarrow 0$  and  $Q(\rho) \rightarrow 0$  when  $\rho \rightarrow 1$ . Then, by solving  $P(Q(\rho) > U) = F\left(1 - \frac{U}{2\pi}\right) = \alpha$ , we have

$$\lambda = -\frac{\log(1 - \alpha)}{\sqrt{-\log\left(\frac{U}{\pi} - \frac{U^2}{4\pi^2}\right)}}. \quad (30)$$

## 4 Simulation Study and Comparisons

The logic behind our proposed prior selection framework lies in checking whether a prior favors simpler models to prevent overfitting. To further illustrate the way of using our framework, and to demonstrate the advantages of employing PC priors for circular models, this section compares the proposed priors in Section 3.2.1 with existing priors from the literature. The comparison focuses on their behavior in both the parameter scale and the distance scale (Section 4.1). Additionally, a comprehensive set of simulation studies is presented in Section 4.2.

### 4.1 Properties of PC and other common priors

In this section we illustrate the behavior of the proposed PC prior as well as other priors from the literature for the three cases models under consideration.

### 4.1.1 Von Mises Distribution

Figure 10 illustrates the behaviors of the PC prior, the popular  $\text{Gamma}(1, b)$  prior,  $h_2$  prior Equation 4, and  $h_3$  prior Equation 4 in both the parameter scale and the distance scale. The distance measure is defined between the von Mises (vM) density and the circular uniform density. For fairness, the scaling parameter  $\lambda$  of the PC prior and the rate parameter  $b$  of the  $\text{Gamma}(1, b)$  prior are calibrated so that both priors share the same median. From the plot of the density on the

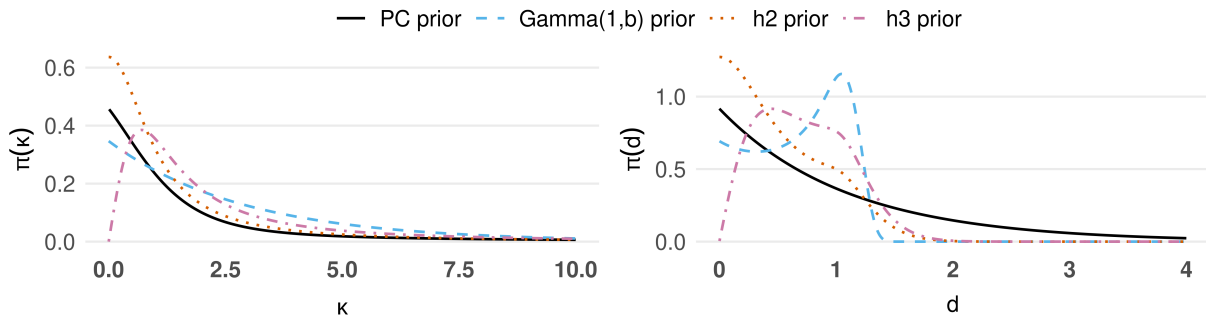


Figure 10: Priors for  $\kappa$  in parameter (left) and distance scale (right) with the base model at  $\kappa_0 = 0$ . The solid line is the PC ( $\lambda = 0.92$ ) prior, the dashed line is the Gamma ( $1, 0.34$ ), the dotted line is the  $h_2$  prior and the dot-dash line is the  $h_3$  prior.

distance scale, it is evident that the  $h_3$  prior assigns zero density at  $d = 0$ , indicating that it never suggests the data being uniform. This behavior leads to overfitting issues. The  $\text{Gamma}(1, b)$  prior has reasonable density at the base model, whereas it exhibits a non-monotonic density with a global maximum around  $d \approx 1$  rather than at  $d = 0$ , which indicates poor robustness in preventing overfitting. The  $h_2$  prior does not penalize the density exponentially with respect to distance by nature; however, it has a reasonable behavior with respect to distance, that is, its density peaks at  $d = 0$  and decreases monotonically as  $d \rightarrow \infty$ . When the base model is at point mass ( $\kappa_0 \rightarrow \infty$ ), Figure 11 reveals that only the PC prior has non-zero density at the simplest case ( $d = 0$ ), whereas the  $\text{Gamma}(1, b)$ ,  $h_2$ , and  $h_3$  priors assign zero density to  $d = 0$ , which makes them ineffective for preventing overfitting in this scenario. Nonetheless, except for the PC prior, the other priors appear to have non-smooth density curve, with 0 density for  $d > 1$ . In

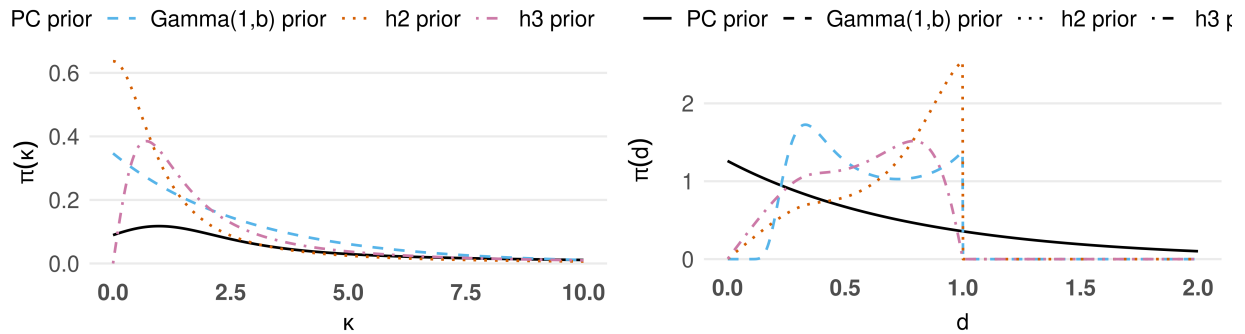


Figure 11: Priors for  $\kappa$  in parameter (left) and distance scale with the base model at  $\kappa_0 \rightarrow \infty$ (right). The solid line is the PC ( $\lambda = 1.26$ ) prior, the dashed line is the Gamma (1, 0.34), the dotted line is the  $h_2$  prior and the dot-dash line is the  $h_3$  prior.

other words, these priors cannot support a model that has moderate distance from the point mass as well.

Recall that the  $h_2$  and  $h_3$  priors are constructed based on the MML criterion, which is intended to penalize model complexity. From the plots given above, we can see that the MML-based priors assign reasonable density to small distances from the base models but do not always allow the model to reach the boundary when the distance measure is defined by Equation 8.

Based on these observations, we recommend using the PC prior for the concentration parameter  $\kappa$  of the von Mises distribution, particularly when limited prior information or belief is available. However, in cases where the data exhibit low concentration, the  $h_2$  prior can also be a reasonable alternative.

#### 4.1.2 Cardioid Distribution

Figure 12 and Figure 13 show the boundary behaviors for the priors for parameter  $\ell$  with the base models being at  $\ell_0 = 0$  and  $\ell_0 \rightarrow 0.5$  respectively. The plots conclude that only PC priors perform well at the boundaries, assigning non-zero density at  $d = 0$ , whilst the density of uniform and  $0.5 \times$  Beta priors are not even smooth. This feature illustrates the possible inherent caveat when priors are specified to be smooth and well-behaved on the parameter scale.

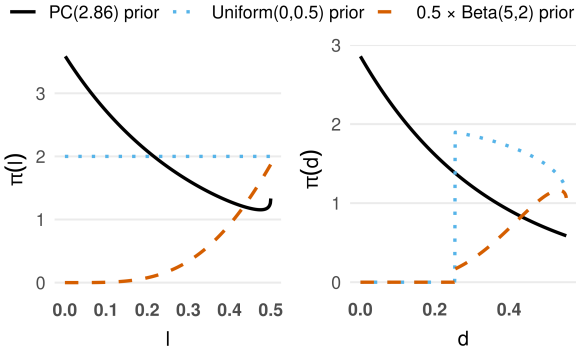


Figure 12: Priors for  $\ell$  in parameter (left) and distance scale with the base model at  $\ell_0 = 0$  (right). The solid line is the PC ( $\lambda = 2.86$ ) prior, the dashed line is the Beta(5, 2) prior and the dotted line is the uniform prior.

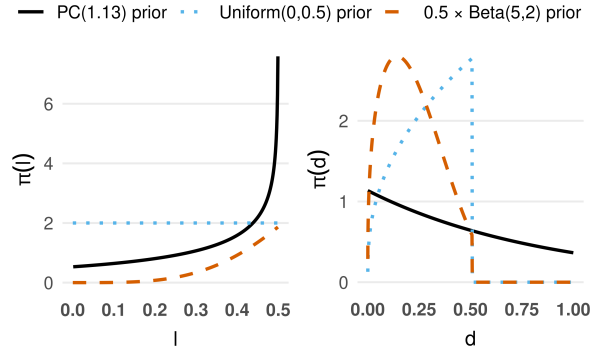


Figure 13: Priors for  $\ell$  in parameter (left) and distance scale with the base model at  $\ell_0 \rightarrow 0.5$  (right). The solid line is the PC ( $\lambda = 1.13$ ) prior, the dashed line is the Beta(5, 2) prior and the dotted line is the uniform prior.

### 4.1.3 Wrapped Cauchy Distribution

The Beta prior is one of the most commonly used choices for the concentration parameter  $\rho$  of the wrapped Cauchy distribution. The prior density on both the parameter scale and the distance scale is illustrated in Figure 14. The behavior of the Beta prior is particularly interesting, as it exhibits different trends near the two boundaries depending on the choice of the  $a$  and  $b$  hyperparameters. The right-hand-side plot shows that the Beta prior can avoid overfitting issues only when  $a < 1$ , ensuring the density at  $d = 0$  is non-zero. Therefore, a Beta prior with  $a < 1$  can be a suitable

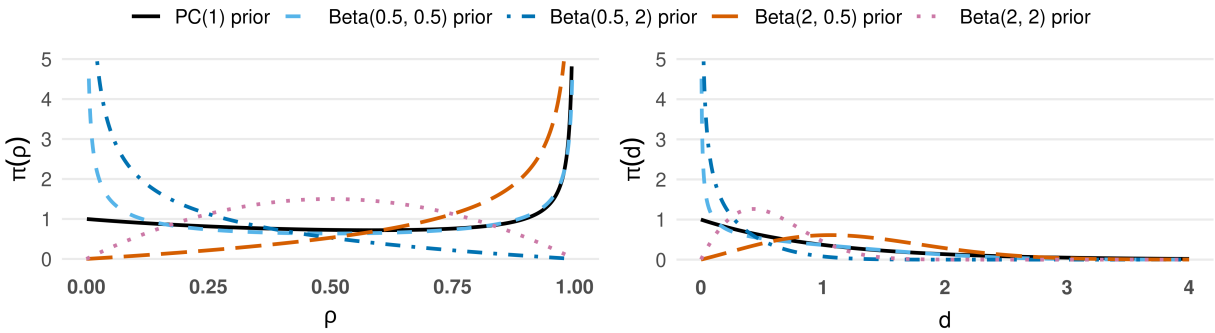


Figure 14: Beta prior and PC ( $\lambda = 1$ ) prior density in parameter ( $p(\rho)$ , left) and distance scale ( $p(d)$ , right).

prior choice for  $\rho$ . When users have sufficient information to set an informative prior, a Beta prior with  $a < 1$  is a reasonable choice, as it maintains the ability to prevent “overconfidence”.

However, selection of the hyperparameter  $b$  significantly influences the behavior of the Beta prior. Thus, we should always be careful when employing this beta prior in practice.

## 4.2 Simulation Study

In former subsections, we illustrate the way of employing our proposed framework, and the behavior of the discussed priors are illustrated and examined. In this section, we further show the performance of the priors and the robustness of the proposed circular PC priors through comprehensive simulation studies. The simulation study is conducted through comparing the posteriors of the concentration parameter  $\xi$  ( $\kappa$  for von Mises distribution,  $\ell$  for cardioid distribution and  $\rho$  for wrapped Cauchy distribution) under different priors. For consistency,  $p(\mu)$  is chosen to be the circular uniform density, thus, the joint posterior is  $p(\mu, \xi | x) \propto p(x | \mu, \xi) p(\mu) p(\kappa)$ .

In the study, posterior samples are obtained using the No-U-Turn Sampler (NUTS), an adaptive variant of Hamiltonian Monte Carlo (HMC), implemented through the Stan interface (Carpenter et al. 2017, Stan Development Team 2025). Sampling is performed using the rstan package version 2.32.7 together with Stan version 2.32.2 to ensure reproducibility. For consistency, the data are sampled from  $p(x | \mu, \xi)$  (vM, cardioid and WC distribution respectively) with  $N = 100, 300, 1000$  sample sizes and location parameter  $\mu = \pi$ . In addition, the result is obtained by averaging over 100 replicates of the experiment. For reproducibility, the random seed is fixed at 520 across all experiments, with individual seeds for the 100 replicates ranging sequentially from 521 to 620. The code used in the simulation study is available at <https://github.com/XiangYEstats/PCpriors-circular>.

The convergence behavior of the model is assessed using the Gelman–Rubin convergence diagnostic,  $\hat{R}$  (Gelman & Rubin 1992) (see details in the *Posterior Analysis* section of Stan Development Team 2025). An  $\hat{R}$  value close to 1 indicates good model convergence. Models

with  $\hat{R} > 1.01$  raise convergence concerns, and  $\hat{R} > 1.1$  is generally considered unacceptable.

#### 4.2.1 Von Mises Distribution

For  $p(\kappa)$  we consider the Gamma  $(1, b)$  (exponential) priors, the  $h_2$  and the  $h_3$  prior (Equation 4, MML priors), and the PC priors with uniform base model (PCU, Equation 12) and point mass base model (PCP, Equation 14). The data for the simulation study are sampled with:  $\kappa =$

0.02, 1, 7, 59; The hyperparameter for Gamma  $(1, b)$  prior has values of  $b = 0.01, 0.05, 0.1, 1, 5;$

The scaling parameters for both PCU and PCP priors are set with  $U = \frac{\pi}{2}$ , and  $\alpha = 0.01, 0.1, 0.3, 0.5, 0.7, 0.9, 0.99.$

The  $\hat{R}$  values for this simulation study are shown in Figure 15. The plots indicate that all priors

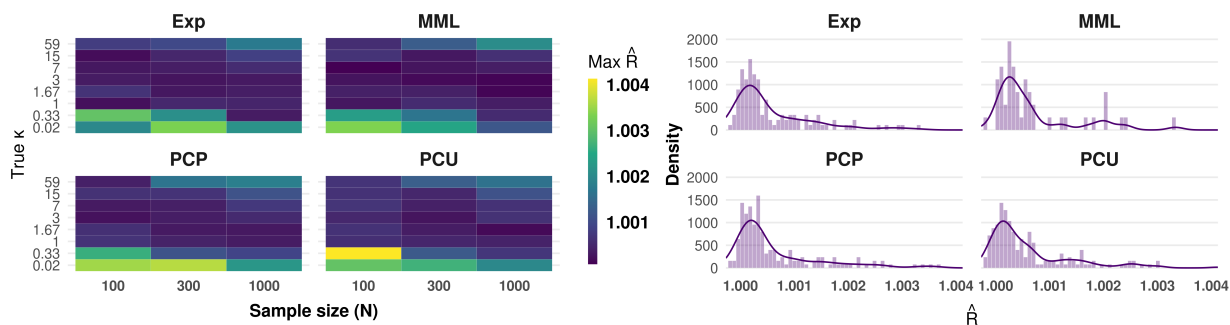


Figure 15:  $\hat{R}$  values for  $\kappa$  in the simulation study. The left plot shows the maximum  $\hat{R}$  for each setting, and the right plot shows the  $\hat{R}$  density by prior. For each setting, the  $\hat{R}$  values for PCU, PCP, and exponential priors are averaged over scaling parameter values, and the  $h_2$  and  $h_3$  priors are averaged and presented under “MML”.

exhibit good convergence behavior when using the Stan model, with the maximum  $\hat{R}$  value being less than 1.004.

From the results in Figure 16, we can see that both PCU and PCP priors perform robustly well with different values of  $\alpha$  (resulting in different values of  $\lambda$ ), whilst the posterior for Gamma  $(1, b)$  priors act differently especially when the sample size is small and the concentration is high. This fact indicates that the Gamma  $(1, b)$  prior highly relies on the value of hyperparameter, whereas the PC priors perform well with different values of  $U$  and  $\alpha$ . Notably, the  $h_2$  prior also performs well in fitting the model. However, based on the discussion in Section 4.1.1, it is not recom-

mended to employ  $h_2$  prior when the data are highly concentrated, as it could overfit the model.

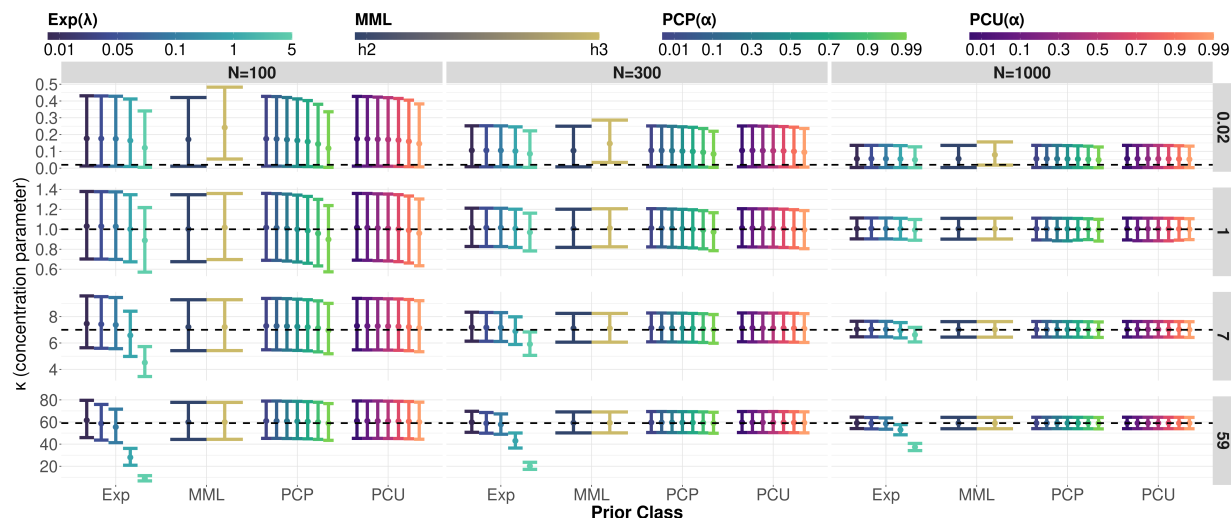


Figure 16: Simulation study for priors on the concentration parameter  $\kappa$  of the von Mises distribution across different sample sizes and true  $\kappa$  values. The horizontal dashed line indicates the true  $\kappa$ , with points showing posterior means and vertical bars indicating 95% posterior credible intervals for each prior class.

#### 4.2.2 Cardioid Distribution

For  $p(\ell)$  we consider the Uniform  $(0, 0.5)$  prior (UNI), the  $0.5 \times \text{Beta}(a, b)$  prior and the PC priors with the uniform base model (PCU, Equation 19) and the cardioid curve base model (PCC, Equation 22). The data are sampled with  $\ell = 0, 0.01, 0.3, 0.49$ ; The hyperparameter for  $0.5 \times \text{Beta}(a, b)$  prior has values of  $a, b \in \{0.5, 1, 2, 5\}$ ; The scaling parameters for both PCC and PCU priors are set with  $U = 0.5$ , but with  $\alpha = 0.01, 0.1, 0.3, 0.5, 0.7, 0.9, 0.99$  for PCC prior and  $\alpha = 0.01, 0.1, 0.2, 0.3, 0.4, 0.5$  for PCU prior, since  $\lambda$  takes very small values when  $\alpha > 0.5$  for PCU prior.

The  $\hat{R}$  values for this simulation study are shown in the left-hand side of Figure 18. The plot shows that the  $0.5 \times \text{Beta}(a, b)$  prior does not converge in the Stan model for large  $\ell$  values and large sample sizes, whereas the Uniform $(0, 0.5)$ , PCC, and PCU priors converge successfully.

From the results given in Figure 17, we could observe that both PCU and PCC priors have much

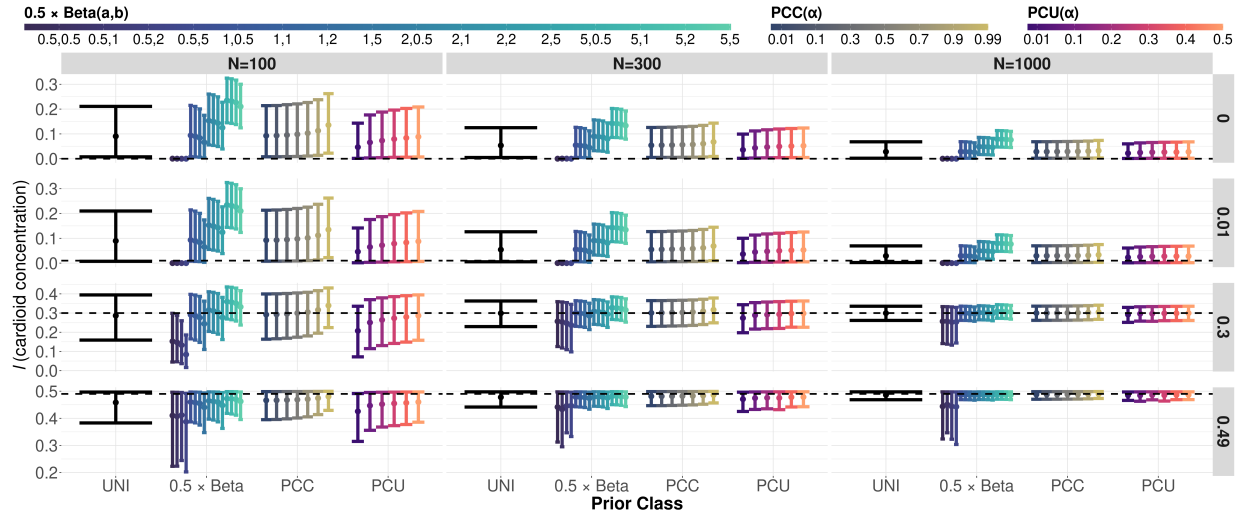


Figure 17: Simulation study for priors on the concentration parameter  $\ell$  of the cardioid distribution across different sample sizes and true  $\ell$  values. The horizontal dashed line indicates the true  $\ell$ , with points showing posterior means and vertical bars indicating 95% posterior credible intervals for each prior class.

more stable and accurate performance than the  $0.5 \times \text{Beta}(a, b)$  prior. Moreover, the PCU prior performs better than the PCC prior around the  $\ell = 0$  boundary, whilst the PCC prior naturally perform better around the  $\ell \rightarrow 0.5$  boundary. This fact demonstrates the importance of base model selection when employing PC prior. In addition, the Uniform  $(0, 0.5)$  prior performs well in our simulation settings, and it is able to recover the true value except when  $\ell = 0$  lies at the boundary. However, as discussed in Section 4.1.2, the Uniform  $(0, 0.5)$  prior does not allocate sufficient density around both base models, and is therefore not recommended, since it may still lead to overfitting. It is worth nothing that almost all priors cannot recover the truth at the  $\ell = 0$  boundary, except for the  $0.5 \times \text{Beta}(a, b)$  prior with  $a < 1$ , and the PCU prior with small  $\alpha$  values (when  $U$  is fixed). This is not surprising since the estimate cannot go below 0 and it is almost impossible to recover the truth if the truth is right at the boundary.

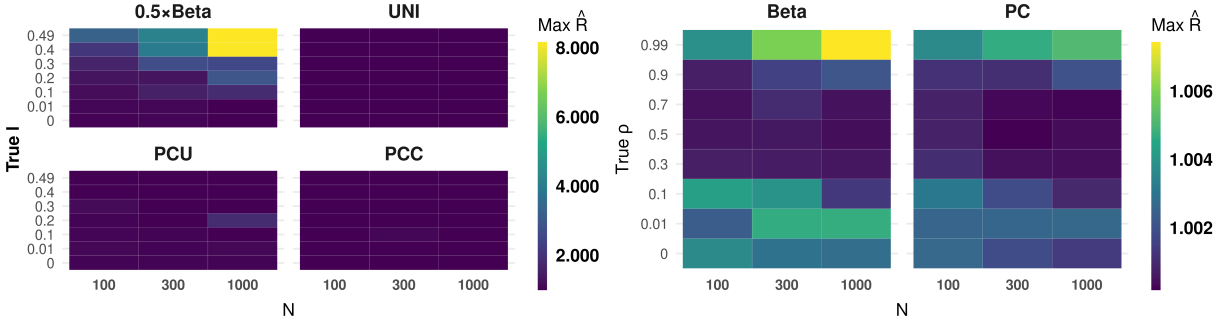


Figure 18:  $\hat{R}$  values for  $\ell$  (left) and  $\rho$  (right) in the simulation study. The plots show the maximum  $\hat{R}$  for each setting. For each setting, the  $\hat{R}$  values for priors with scaling parameter are averaged over scaling parameter values.

### 4.2.3 Wrapped Cauchy Distribution

For  $p(\rho)$  we consider the Beta ( $a, b$ ) and the PC priors (Equation 28). The data are sampled with  $\rho = 0, 0.01, 0.5, 0.99$ ; The hyperparameter for Beta ( $a, b$ ) prior has values of  $a, b \in \{0.5, 1, 2, 5\}$ ; The scaling parameters for PC prior are set with  $U = 0.6$ , and  $\alpha = 0.01, 0.1, 0.3, 0.5, 0.7, 0.9, 0.99$ . The right-hand side plot in Figure 18 shows that both priors achieve good convergence, while the PC prior has slightly lower  $\hat{R}$  values when the true  $\rho$  is close to either boundary.

Figure 19 shows that the PC priors demonstrate more stable and accurate performance than the Beta ( $a, b$ ) prior. However, if sufficient prior information supports the use of a Beta ( $a, b$ ) prior, as discussed in Section 4.1.3, we suggest that Beta ( $a, b$ ) prior with  $a < 1$  are appropriate choices, since they do not lead to overfitting issues. This behavior is also evident in Figure 19. For simulation setting with  $\rho = 0$ , the Beta ( $a, b$ ) prior with  $a = 0.5$  produces reasonable estimates, with the credible interval successfully recovering the boundary base model. Through the comparative study presented in this section, we have illustrated our strategy for selecting priors that effectively prevent overfitting in circular distributions, emphasizing that the PC prior is consistently an appropriate choice. We acknowledge that some other priors may also perform acceptably in preventing overfitting and may even outperform the PC prior when sufficient information is available to set an informative prior as expected. However, given the fact that the

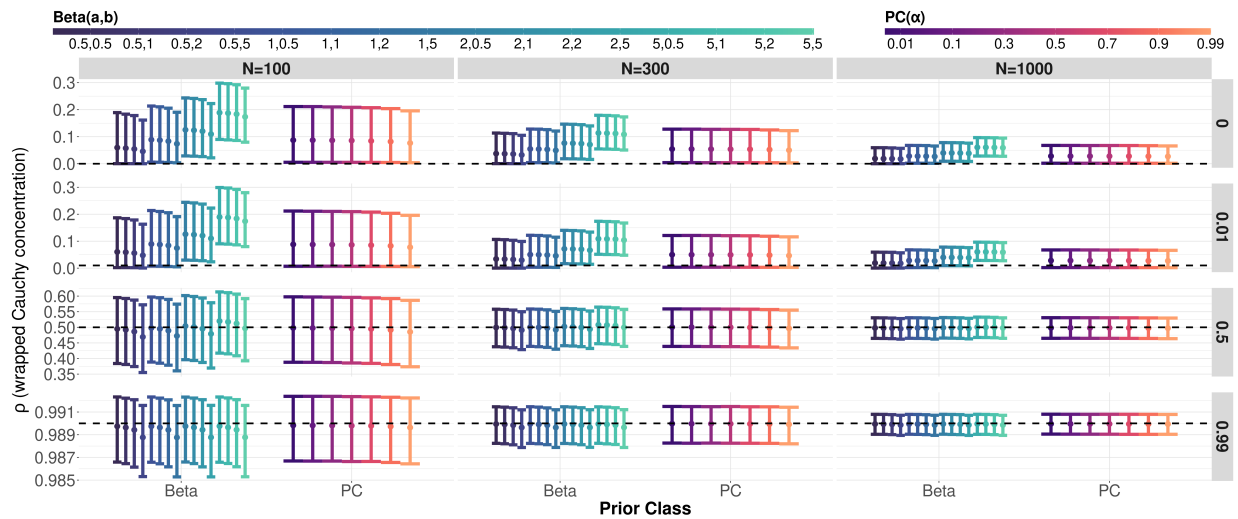


Figure 19: Simulation study for priors on the concentration parameter  $\rho$  of the wrapped Cauchy distribution across different sample sizes and true  $\rho$  values. The horizontal dashed line indicates the true  $\rho$ , with points showing posterior means and vertical bars indicating 95% posterior credible intervals for each prior class.

procedure outlined in the previous sections has manifested the special efficacy of the adapted framework in selecting priors which can effectively prevent overfitting in circular distributions, it is hence highly recommended that this procedure be employed to carefully examine the behavior of the chosen prior in the distance scale so as to prevent its overfitting.

## 5 Application

In this section, we present a real-data case study to show the practical performance of the discussed priors. The data used in this study are the `wind` data (Figure 20) stored in “circular” package (Lund et al. 2017) in R, recorded by a meteorological station in a place named “Col de la Roa” in the Italian Alps. The dataset contains 310 measures of daily wind direction from January 29th, 2001 to March 31st, 2001 covering the data span from 3 a.m. to 4 a.m. of the day. As a circular analogue of normal distribution, von Mises distribution is employed for our model, and the Bayesian model is the same as expressed in Section 4.2. For comparison, the Stan model with  $p(\kappa)$  being PC prior, Gamma  $(1, b)$  prior (exponential prior),  $h_2$  prior and  $h_3$  prior for  $\kappa$  are

constructed.

We choose  $b = 0.1, 1, 2, 5, 10$  for the Gamma  $(1, b)$  prior. From Figure 20, we can observe that this dataset is not highly concentrated. Therefore, for the PC prior, the circular uniform base model would be a more natural choice compared with the point mass base model. However, the purpose of comparison and illustration, models with PC prior with both base models are constructed. We choose the scaling parameter  $\lambda$  following the procedure discussed in Section 3.1 with  $U = \pi, \frac{\pi}{2}, \frac{\pi}{4}, \frac{\pi}{8}, \frac{\pi}{16}$ , indicating different radians around  $x = 0$ . The  $\alpha$  value is computed by finding ratio between the number of data lying in the chosen radian  $U$  and 310 (total amount of data). After fitting the model, the posterior mean and the 95% credible interval for  $\kappa$  are given

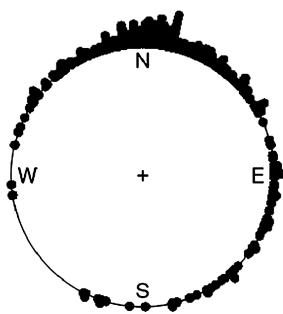


Figure 20: Wind data.

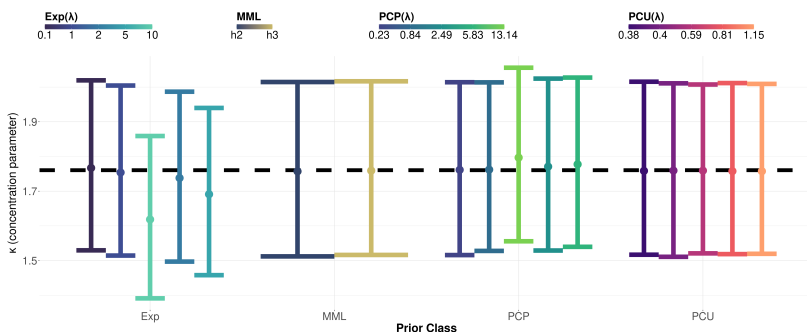


Figure 21: Posterior means and credible intervals of  $\kappa$ .

Table 1: Model comparison metrics for von Mises priors. Lower WAIC/LOOIC/DIC and higher ELPD indicate better predictive performance.

Metric	Exp( $\lambda$ )					MML		PCP( $\lambda$ )					PCU( $\lambda$ )					
	0.10	1.00	2.00	5.00	10.00	$h_2$	$h_3$	0.23	0.84	2.49	5.83	13.14	0.38	0.40	0.59	0.81	1.15	
WAIC	838.29	838.29	838.41	838.59	839.61	838.47	838.35	838.35	838.27	838.34	838.34	838.34	838.38	838.27	838.44	<b>838.22</b>	838.31	838.34
LOOIC	838.29	838.30	838.41	838.59	839.61	838.47	838.35	838.36	838.28	838.35	838.34	838.38	838.27	838.44	<b>838.22</b>	838.31	838.34	
ELPD	-419.15	-419.15	-419.20	-419.29	-419.80	-419.23	-419.17	-419.18	-419.14	-419.17	-419.17	-419.19	-419.13	-419.22	<b>-419.11</b>	-419.15	-419.17	
DIC	836.10	836.13	836.22	836.51	837.59	836.19	836.14	836.14	836.11	836.13	836.12	836.15	836.11	836.18	<b>836.09</b>	836.13	836.14	

in Figure 21. In the plot, the horizontal dashed line indicates the frequentist maximum likelihood estimate of  $\kappa$ , with points showing posterior means and vertical bars indicating 95% posterior credible intervals for each prior class. From the plot, the PC prior with circular uniform base model (PCU) and PC prior with point mass base model (PCP) fit the data well in terms of the

stability of credible interval and posterior mean. For this dataset, as a more natural choice, the PCU prior is indeed robust than PCP prior, since the value of scaling parameter  $\lambda$  does not vary much with the same given  $U$  and  $\alpha$  values.

The model comparison metrics are given in Table 1. The Watanabe–Akaike Information Criterion (WAIC) (Watanabe & Opper 2010), Leave-One-Out Information Criterion (LOOIC) (Vehtari et al. 2017), Expected Log Predictive Density (ELPD) and Deviance Information Criterion (DIC) (Spiegelhalter et al. 2002) are employed for assessing the prior performance in same model. The PCU (0.59) prior performs the best among all priors according to the score of all metrics. The other PCU and PCP priors show robustness, compared with the Gamma(1,  $b$ ) (Exp) prior, as the most extreme values for  $\lambda$  in our example still lead to good model comparison metrics values, whereas Figure 21 shows that the posterior mean and credible interval of Exp prior is quite sensitive to the  $\lambda$  values, but there is insufficient guidance for choosing the values for hyperparameters of Gamma(1,  $b$ ) prior. In addition, the  $h_2$  and  $h_3$  priors both perform well in this example. In Section 4.1.1, we discussed that  $h_2$  prior also performs well in preventing overfitting when the base model is the circular uniform distribution. Thus, to prevent overfitting, the  $h_2$  prior also appears to be a proper choice of prior for  $\kappa$  when the data appear to have low concentration.

This practical example further demonstrates that the PC priors have stable and comparable performance in circular scenarios. Therefore, employing PC prior for Bayesian circular models not only prevents overfitting but also produces accurate results.

## 6 Conclusion and Outlook

A principled framework for selecting priors for parameters of circular distributions is essential for constructing robust Bayesian circular models and for avoiding overfitting as model complex-

ity increases. The framework proposed in this paper focuses on assessing whether a prior can properly guard against overfitting, thereby supporting a more reliable construction of Bayesian circular models. Additionally, it provides a simple and practical way to choose prior hyperparameters so that the resulting priors can be either strongly or weakly informative, depending on the level of prior knowledge available.

The derived priors are inherently designed to prevent overfitting and remain robust choices even when sufficient information is available. However, they may not always be the most appropriate choice in such cases, as more informative priors tailored to specific scenarios could perform better. In these situations, the proposed framework can be employed to rigorously evaluate model complexity and ensure the appropriateness of alternative priors. It is worth noting that the present analysis does not include a direct numerical diagnostic for prior overfitting. Instead, overfitting is assessed theoretically by examining whether a prior places sufficient mass near the chosen base model, which is clearly observed when representing the prior on the distance scale. While a dedicated quantitative metric could further support this assessment, introducing such tools is beyond the scope of this work and may be explored in future research.

With prior selection strategies addressed in this work, the next step involves developing general and intuitive procedures for constructing a variety of Bayesian circular models, including those with circular covariates, circular responses, or both. Future efforts will also focus on extending the framework to accommodate joint priors and providing conditional PC priors, which are vital for handling multi-parameter and multi-modal distributions and models.

## **Supplementary materials**

The supplementary materials include the appendix for the derivation of the PC priors, and the code for simulation studies (in `ibex cluster`) and application (in `R`). They are available at [https :](https://)

## A Appendix: Derivation of PC Priors

### A.1 The PC Prior for the Concentration Parameter of Von Mises Distribution

#### A.1.1 With Circular Uniform Base Model

With the base model is at  $\kappa_0 = 0$ , then the KLD in Equation 11 becomes

$$\text{KLD}(\mathcal{VM}||\mathcal{VM}_0) |_{\kappa_0=0} = \frac{\kappa \mathcal{I}_1(\kappa)}{\mathcal{I}_0(\kappa)} - \log(\mathcal{I}_0(\kappa)). \quad (31)$$

Then, the distance is

$$d(\kappa) = \sqrt{\frac{\kappa \mathcal{I}_1(\kappa)}{\mathcal{I}_0(\kappa)} - \log(\mathcal{I}_0(\kappa))}, \quad (32)$$

and its derivative is

$$\frac{\partial d(\kappa)}{\partial \kappa} = \frac{\frac{\kappa(\mathcal{I}_0(\kappa) + \mathcal{I}_2(\kappa))}{2\mathcal{I}_0(\kappa)} - \frac{\kappa \mathcal{I}_1(\kappa)^2}{\mathcal{I}_0(\kappa)^2}}{2d(\kappa)}, \quad (33)$$

which is positive for  $\kappa \in [0, \infty)$ . Thus,

$$\begin{aligned} \pi(\kappa) &= \lambda \exp\{-\lambda d(\kappa)\} \left| \frac{\partial d(\kappa)}{\partial \kappa} \right| = \lambda \exp\{-\lambda d(\kappa)\} \frac{\frac{\kappa(\mathcal{I}_0(\kappa) + \mathcal{I}_2(\kappa))}{2\mathcal{I}_0(\kappa)} - \frac{\kappa \mathcal{I}_1(\kappa)^2}{\mathcal{I}_0(\kappa)^2}}{2d(\kappa)} \\ &= \lambda \exp\left\{-\lambda \sqrt{\frac{\kappa \mathcal{I}_1(\kappa)}{\mathcal{I}_0(\kappa)} - \log(\mathcal{I}_0(\kappa))}\right\} \frac{\frac{\kappa(\mathcal{I}_0(\kappa) + \mathcal{I}_2(\kappa))}{2\mathcal{I}_0(\kappa)} - \frac{\kappa \mathcal{I}_1(\kappa)^2}{\mathcal{I}_0(\kappa)^2}}{2\sqrt{\frac{\kappa \mathcal{I}_1(\kappa)}{\mathcal{I}_0(\kappa)} - \log(\mathcal{I}_0(\kappa))}}, \end{aligned} \quad (34)$$

which is given in Proposition 3.1.

### A.1.2 With Point Mass Base Model

If  $\kappa_0 \gg \kappa$  is chosen as the base model, we derive the corresponding PC prior following the approach given in Appendix A.1 of [Simpson et al. \(2017\)](#). The derivation start with approximating the KLD using an asymptotic expansion for  $\log(\mathcal{I}_0(\kappa_0))$  as  $\kappa_0 \rightarrow \infty$ :

$$\log(\mathcal{I}_0(\kappa_0)) \stackrel{\kappa_0 \rightarrow \infty}{\sim} \kappa_0 - \frac{1}{2} \log(2\pi) - \frac{1}{2} \log(\kappa_0) + \frac{1}{8\kappa_0} + \mathcal{O}\left(\frac{1}{\kappa_0^2}\right). \quad (35)$$

Therefore,

$$\begin{aligned} \frac{\text{KLD}(\mathcal{VM} \parallel \mathcal{VM}_0)}{\kappa_0} &\stackrel{\kappa_0 \rightarrow \infty}{\sim} -\frac{\log(\mathcal{I}_0(\kappa))}{\kappa_0} + \frac{\log(\mathcal{I}_0(\kappa_0))}{\kappa_0} + (\kappa - \kappa_0) \frac{\mathcal{I}_1(\kappa)}{\kappa_0 \mathcal{I}_0(\kappa)} \\ &= 1 - \frac{\mathcal{I}_1(\kappa)}{\mathcal{I}_0(\kappa)} + \mathcal{O}\left(\frac{1}{\kappa_0^2}\right). \end{aligned} \quad (36)$$

Notice that for any PC prior with the KLD in the form of  $\frac{\text{KLD}}{g(\xi_0)} = h(\xi)$  where  $g(\xi_0)$  is a function of  $\xi_0$  and  $h(\xi)$  is a function of  $\xi$ , by setting  $d(\xi) = \sqrt{h(\xi)}$ , we can re-define the PC prior density as

$$d(\xi) = \tilde{\lambda} \exp \left\{ -\tilde{\lambda} \frac{d(\xi)}{\sqrt{g(\xi_0)}} \right\} \left| \frac{1}{\sqrt{g(\xi_0)}} \frac{\partial d(\xi)}{\partial \xi} \right|. \quad (37)$$

Then, with  $\lambda = \frac{\tilde{\lambda}}{\sqrt{g(\xi_0)}}$ , this formulation is equivalent to Equation 9.

For the KLD given in Equation 36,  $g(\kappa_0) = \kappa_0$ , and  $h(\kappa) = 1 - \frac{\mathcal{I}_1(\kappa)}{\mathcal{I}_0(\kappa)}$ . Thus, the distance is

$$d(\kappa) = \sqrt{1 - \frac{\mathcal{I}_1(\kappa)}{\mathcal{I}_0(\kappa)}}, \quad (38)$$

and its derivative is

$$\frac{\partial d(\kappa)}{\partial \kappa} = \frac{\left( \frac{\mathcal{I}_1(\kappa)^2}{\mathcal{I}_0(\kappa)^2} - \frac{\mathcal{I}_0(\kappa) + \mathcal{I}_2(\kappa)}{2\mathcal{I}_0(\kappa)} \right)}{2d(\kappa)}, \quad (39)$$

which is negative for  $\kappa \in [0, \infty)$ . The derivation of the pdf of this PC prior (Proposition 3.2)

is then given below:

$$\begin{aligned} \pi(\kappa) &= \tilde{\lambda} \exp \left\{ -\tilde{\lambda} \frac{d(\kappa)}{\sqrt{\kappa_0}} \right\} \left| \frac{1}{\sqrt{\kappa_0}} \frac{\partial d(\kappa)}{\partial \kappa} \right| = \lambda \exp \{ -\lambda d(\kappa) \} \frac{\left( \frac{\mathcal{I}_0(\kappa) + \mathcal{I}_2(\kappa)}{2\mathcal{I}_0(\kappa)} - \frac{\mathcal{I}_1(\kappa)^2}{\mathcal{I}_0(\kappa)^2} \right)}{2d(\kappa)} \\ &= \lambda \exp \left\{ \lambda \sqrt{1 - \frac{\mathcal{I}_1(\kappa)}{\mathcal{I}_0(\kappa)}} \right\} \frac{\left( \frac{\mathcal{I}_0(\kappa) + \mathcal{I}_2(\kappa)}{2\mathcal{I}_0(\kappa)} - \frac{\mathcal{I}_1(\kappa)^2}{\mathcal{I}_0(\kappa)^2} \right)}{2\sqrt{1 - \frac{\mathcal{I}_1(\kappa)}{\mathcal{I}_0(\kappa)}}}, \end{aligned} \quad (40)$$

where  $\lambda = \frac{\tilde{\lambda}}{\sqrt{\kappa_0}}$ .

## A.2 The PC Prior for the Concentration Parameter of Cardioid Distribution

### A.2.1 With Circular Uniform Base Model

With the circular uniform base model ( $\ell_0 = 0$ ), approximating KLD through asymptotic expansion with respect to  $\ell_0$  yields

$$-\frac{\ell}{\ell_0} \left( 1 - \sqrt{1 - 4\ell_0^2} \right) \stackrel{\ell_0 \rightarrow 0^+}{\sim} -\ell (2\ell_0 + 2\ell_0^3) + \mathcal{O}(\ell_0^4) = 0, \quad (41)$$

and

$$\frac{1}{2} \log \left( 1 - \sqrt{1 - 4\ell_0^2} \right) \stackrel{\ell_0 \rightarrow 0^+}{\sim} \frac{\log(2)}{2} + \log(\ell_0) + \frac{1}{2}\ell_0^2 + \mathcal{O}(\ell_0^4). \quad (42)$$

Substituting them into Equation 18, we obtain

$$\text{KLD}(\mathcal{C} \parallel \mathcal{C}_0) \stackrel{\ell_0 \rightarrow 0^+}{\sim} 1 - \sqrt{1 - 4\ell^2} + \log(\ell) + \frac{1}{2} \log \left( \frac{1 + \sqrt{1 - 4\ell^2}}{1 - \sqrt{1 - 4\ell^2}} \right) + \mathcal{O}(\ell^4), \quad (43)$$

and the distance is therefore

$$d(\ell) = \sqrt{\left(1 - \sqrt{1 - 4\ell^2} + \log(\ell) + \frac{1}{2} \log\left(\frac{1 + \sqrt{1 - 4\ell^2}}{1 - \sqrt{1 - 4\ell^2}}\right)\right)}. \quad (44)$$

Thus,

$$\frac{\partial d(\ell)}{\partial \ell} = \frac{2\ell}{(1 + \sqrt{1 - 4\ell^2}) d(\ell)}, \quad (45)$$

which is positive for  $\ell \in [0, \frac{1}{2})$ . Therefore,

$$\pi(\ell) = \lambda \exp\{-\lambda d(\ell)\} \left| \frac{\partial d(\ell)}{\partial \ell} \right| = \lambda \exp\{-\lambda d(\ell)\} \frac{2\ell}{(1 + \sqrt{1 - 4\ell^2}) d(\ell)}. \quad (46)$$

The support for  $\ell$  is  $[0, \frac{1}{2})$ , whilst the support for the variable of an exponential distribution is  $[0, \infty)$ . Thus, an additional normalizing constant is required and is given by:

$$\int_0^{\frac{1}{2}} \pi(\ell) d\ell = 1 - \exp\left\{-\lambda \sqrt{1 - \log(2)}\right\}. \quad (47)$$

The CDF for this PC prior is

$$F(\ell) = \frac{\int \pi(\ell) d\ell}{\int_0^{\frac{1}{2}} \pi(\ell) d\ell} = \frac{1 - \exp\left\{-\lambda \sqrt{1 - \sqrt{1 - 4\ell^2} + \log(\ell) + \frac{1}{2} \log\left(\frac{1 + \sqrt{1 - 4\ell^2}}{1 - \sqrt{1 - 4\ell^2}}\right)}\right\}}{1 - \exp\left\{-\lambda \sqrt{1 - \log(2)}\right\}}. \quad (48)$$

Therefore, the exact expression for the pdf of this PC prior is

$$\pi(\ell) = \frac{\partial F(\ell)}{\partial \ell} = \lambda \exp\{-\lambda d(\ell)\} \frac{2\ell \exp\left\{\lambda \sqrt{1 - \log(2)}\right\}}{\left(\exp\left\{\lambda \sqrt{1 - \log(2)}\right\} - 1\right) (1 + \sqrt{1 - 4\ell^2}) d(\ell)}. \quad (49)$$

### A.2.2 With Cardioid Curve Base Model

When the base model is at  $\ell_0 \rightarrow \frac{1}{2}$ ,

$$\lim_{\ell_0 \rightarrow \frac{1}{2}} \text{KLD}(\mathcal{C} \parallel \mathcal{C}_0) = 1 + \log(2) - 2\ell - \sqrt{1 - 4\ell^2} + \log(\ell) + \frac{1}{2} \log\left(\frac{1 + \sqrt{1 - 4\ell^2}}{1 - \sqrt{1 - 4\ell^2}}\right). \quad (50)$$

Therefore,

$$d(\ell) = \sqrt{1 + \log(2) - 2\ell - \sqrt{1 - 4\ell^2} + \log(\ell) + \frac{1}{2} \log\left(\frac{1 + \sqrt{1 - 4\ell^2}}{1 - \sqrt{1 - 4\ell^2}}\right)}, \quad (51)$$

and the derivative is

$$\frac{\partial d(\ell)}{\partial \ell} = -\frac{2\ell + \sqrt{1 - 4\ell^2} - 1}{2\ell d(\ell)}, \quad (52)$$

which is negative for  $\ell \in [0, \frac{1}{2})$ . Thus,

$$\pi(\ell) = \lambda \exp\{-\lambda d(\ell)\} \left| \frac{\partial d(\ell)}{\partial \ell} \right| = \lambda \exp\{-\lambda d(\ell)\} \frac{2\ell + \sqrt{1 - 4\ell^2} - 1}{2\ell d(\ell)}. \quad (53)$$

For this PC prior, the normalizing constant is

$$\int_0^{\frac{1}{2}} \pi(\ell) d\ell = 1. \quad (54)$$

Therefore, the CDF is

$$F(\ell) = \exp\{-\lambda d(\ell)\}, \quad (55)$$

and the density remains to be

$$\pi(\ell) = \lambda \exp\{-\lambda d(\ell)\} \frac{2\ell + \sqrt{1 - 4\ell^2} - 1}{2\ell d(\ell)}. \quad (56)$$

### A.3 The PC Prior for the Concentration Parameter of Wrapped Cauchy Distribution

From Equation 27, the distance is

$$d(\rho) = \sqrt{-\log(1 - \rho^2)}, \quad (57)$$

and its derivative is

$$\frac{\partial d(\rho)}{\partial \rho} = \frac{\rho}{(1 - \rho^2) \sqrt{-\log(1 - \rho^2)}} = \frac{\rho}{(1 - \rho^2) d(\rho)}, \quad (58)$$

which is positive for  $\rho \in [0, 1)$ . Therefore, the density is

$$\begin{aligned} \pi(\rho) &= \lambda \exp\{-\lambda d(\rho)\} \left| \frac{\partial d(\rho)}{\partial \rho} \right| = \lambda \exp\{-\lambda d(\rho)\} \frac{\rho}{(1 - \rho^2) d(\rho)} \\ &= \lambda \exp\left\{-\lambda \sqrt{-\log(1 - \rho^2)}\right\} \frac{\rho}{(1 - \rho^2) \sqrt{-\log(1 - \rho^2)}}. \end{aligned} \quad (59)$$

Since the normalizing constant is  $\int_0^1 \pi(\rho) d\rho = 1$ , the density remain the same.

In addition, to derive the expression of the beta prior in terms of distance scale, we rewrite Equation 57 as Equation 60.

$$\rho(d) = \sqrt{1 - \exp\{-d^2\}}. \quad (60)$$

Therefore,

$$\begin{aligned}
\pi(d) &= \frac{\Gamma(a+b)}{\Gamma(a)\Gamma(b)} \rho(d)^{a-1} (1-\rho(d))^{b-1} \left| \frac{\partial \rho(d)}{\partial d} \right| \\
&= \frac{\Gamma(a+b)}{\Gamma(a)\Gamma(b)} \left( \sqrt{1-\exp\{-d^2\}} \right)^{a-1} \left( 1 - \sqrt{1-\exp\{-d^2\}} \right)^{b-1} \frac{d \exp\{-d^2\}}{\sqrt{1-\exp\{-d^2\}}}.
\end{aligned} \tag{61}$$

## References

- Banerjee, A., Dhillon, I. S., Ghosh, J., Sra, S. & Ridgeway, G. (2005), ‘Clustering on the unit hypersphere using von mises-fisher distributions.’, *Journal of Machine Learning Research* **6**(9).
- Boomsma, W., Mardia, K. V., Taylor, C. C., Ferkinghoff-Borg, J., Krogh, A. & Hamelryck, T. (2008), ‘A generative, probabilistic model of local protein structure’, *Proceedings of the National Academy of Sciences* **105**(26), 8932–8937.
- Cabella, P. & Marinucci, D. (2009), ‘Statistical challenges in the analysis of cosmic microwave background radiation’, *The Annals of Applied Statistics* .
- Cabral, R., Bolin, D. & Rue, H. (2023), ‘Controlling the flexibility of non-gaussian processes through shrinkage priors’, *Bayesian Analysis* **18**(4), 1223–1246.
- Carpenter, B., Gelman, A., Hoffman, M. D., Lee, D., Goodrich, B., Betancourt, M., Brubaker, M., Guo, J., Li, P. & Riddell, A. (2017), ‘Stan: A probabilistic programming language’, *Journal of statistical software* **76**, 1–32.
- Damien, P. & Walker, S. (1999), ‘A full bayesian analysis of circular data using the von mises distribution’, *The Canadian Journal of Statistics/La Revue Canadienne de Statistique* pp. 291–298.

- Dhillon, I. S. & Modha, D. S. (2001), 'Concept decompositions for large sparse text data using clustering', *Machine learning* **42**(1), 143–175.
- Dowe, D. L., Oliver, J. J., Baxter, R. A. & Wallace, C. S. (1996), Bayesian estimation of the von mises concentration parameter, in 'Maximum Entropy and Bayesian Methods: Santa Fe, New Mexico, USA, 1995 Proceedings of the Fifteenth International Workshop on Maximum Entropy and Bayesian Methods', Springer, pp. 51–60.
- Esteves, C., Allen-Blanchette, C., Makadia, A. & Daniilidis, K. (2018), Learning so (3) equivariant representations with spherical cnns, in 'Proceedings of the european conference on computer vision (ECCV)', pp. 52–68.
- Fuglstad, G.-A., Simpson, D., Lindgren, F. & Rue, H. (2019), 'Constructing priors that penalize the complexity of gaussian random fields', *Journal of the American Statistical Association* **114**(525), 445–452.
- Gelman, A. & Rubin, D. B. (1992), 'Inference from iterative simulation using multiple sequences', *Statistical science* **7**(4), 457–472.
- Gumbel, E., Greenwood, J. A. & Durand, D. (1953), 'The circular normal distribution: Theory and tables', *Journal of the American Statistical Association* **48**(261), 131–152.
- Guttorp, P. & Lockhart, R. A. (1988), 'Finding the location of a signal: A bayesian analysis', *Journal of the American Statistical Association* **83**(402), 322–330.
- Jammalamadaka, S. (2001), *Topics in Circular Statistics*, Vol. 336, World Scientific.
- Jones, M. & Pewsey, A. (2005), 'A family of symmetric distributions on the circle', *Journal of the American Statistical Association* **100**(472), 1422–1428.

- Jung, S., Foskey, M. & Marron, J. (2011), ‘Principal arc analysis on direct product manifolds’, *The Annals of Applied Statistics* .
- Kato, S. & Jones, M. (2010), ‘A family of distributions on the circle with links to, and applications arising from, möbius transformation’, *Journal of the American Statistical Association* **105**(489), 249–262.
- Kullback, S. & Leibler, R. A. (1951), ‘On information and sufficiency’, *The annals of mathematical statistics* **22**(1), 79–86.
- Ley, C. & Verdebout, T. (2017), *Modern directional statistics*, Chapman and Hall/CRC.
- Lund, U., Agostinelli, C. & Agostinelli, M. C. (2017), ‘Package ‘circular’’, *Repository CRAN* **775**(5), 20–135.
- Mardia, K. V., Foldager, J. I. & Frellsen, J. (2018), Directional statistics in protein bioinformatics, in ‘Applied Directional Statistics’, Chapman and Hall/CRC, pp. 17–40.
- Mardia, K. V. & Jupp, P. E. (2009), *Directional statistics*, John Wiley & Sons.
- Marinucci, D. & Peccati, G. (2011), *Random fields on the sphere: representation, limit theorems and cosmological applications*, Vol. 389, Cambridge University Press.
- Marrelec, G. & Giron, A. (2024), ‘Estimating the concentration parameter of a von mises distribution: a systematic simulation benchmark’, *Communications in Statistics-Simulation and Computation* **53**(1), 117–129.
- Nuñez-Antonio, G., Gutiérrez-Peña, E. & Escarela, G. (2011), ‘A bayesian regression model for circular data based on the projected normal distribution’, *Statistical Modelling* **11**(3), 185–201.

- Pardo, A., Real, E., Krishnaswamy, V., López-Higuera, J. M., Pogue, B. W. & Conde, O. M. (2016), 'Directional kernel density estimation for classification of breast tissue spectra', *IEEE Transactions on Medical Imaging* **36**(1), 64–73.
- Pewsey, A. & García-Portugués, E. (2021), 'Recent advances in directional statistics', *Test* **30**(1), 1–58.
- Ravindran, P. & Ghosh, S. K. (2011), 'Bayesian analysis of circular data using wrapped distributions', *Journal of Statistical Theory and Practice* **5**(4), 547–561.
- Rodriguez Avellaneda, F., Chacón-Montalván, E. A. & Moraga, P. (2025), 'Multivariate disaggregation modeling of air pollutants: a case-study of pm2.5, pm10 and ozone prediction in portugal and italy', *The American Statistician* pp. 1–26.
- Simpson, D., Rue, H., Riebler, A., Martins, T. G. & Sørbye, S. H. (2017), 'Penalising model component complexity: A principled, practical approach to constructing priors', *Statistical Science* .
- Sørbye, S. H. & Rue, H. (2017), 'Penalised complexity priors for stationary autoregressive processes', *Journal of Time Series Analysis* **38**(6), 923–935.
- Spiegelhalter, D. J., Best, N. G., Carlin, B. P. & Van Der Linde, A. (2002), 'Bayesian measures of model complexity and fit', *Journal of the royal statistical society: Series b (statistical methodology)* **64**(4), 583–639.
- Sra, S. (2016), 'Directional statistics in machine learning: a brief review', *Applied Directional Statistics* .
- Stan Development Team (2025), 'RStan: the R interface to Stan'. R package version 2.32.7.  
**URL:** <https://mc-stan.org/>

- Van Niekerk, J., Bakka, H. & Rue, H. (2021), ‘A principled distance-based prior for the shape of the weibull model’, *Statistics & Probability Letters* **174**, 109098.
- Vehtari, A., Gelman, A. & Gabry, J. (2017), ‘Practical bayesian model evaluation using leave-one-out cross-validation and waic’, *Statistics and computing* **27**(5), 1413–1432.
- Ventrucci, M. & Rue, H. (2016), ‘Penalized complexity priors for degrees of freedom in bayesian p-splines’, *Statistical Modelling* **16**(6), 429–453.
- Vuollo, V., Holmström, L., Aarnivala, H., Harila, V., Heikkinen, T., Pirttiniemi, P. & Valkama, A. M. (2016), ‘Analyzing infant head flatness and asymmetry using kernel density estimation of directional surface data from a craniofacial 3d model’, *Statistics in medicine* **35**(26), 4891–4904.
- Wallace, C. & Dowe, D. L. (1993), *MML estimation of the von Mises concentration parameter*, Monash University, Department of Computer Science.
- Watanabe, S. & Opper, M. (2010), ‘Asymptotic equivalence of bayes cross validation and widely applicable information criterion in singular learning theory.’, *Journal of machine learning research* **11**(12).